

CALIFORNIA INSTITUTE OF TECHNOLOGY

EARTHQUAKE ENGINEERING RESEARCH LABORATORY

DRIFT DEMAND SPECTRA FOR
SELECTED NORTHRIDGE SITES

BY

WILFRED D. IWAN

REPORT NO. EERL 95-07

A REPORT ON RESEARCH CONDUCTED UNDER A SUBCONTRACT
FROM SAC JOINT VENTURE

FUNDED BY
THE FEDERAL EMERGENCY MANAGEMENT AGENCY (FEMA)

PASADENA, CALIFORNIA
DECEMBER 1995

Drift Demand Spectra for Selected Northridge Sites

by

Wilfred D. Iwan

Report No. EERL 95-07

A Report on Research Conducted Under a Subcontract
from SAC Joint Venture

SAC Joint Venture: A partnership of
the Structural Engineers Association,
the Applied Technology Council, and
the California Universities for Research in
Earthquake Engineering

Funded by
the Federal Emergency Management Agency (FEMA)

California Institute of Technology
Pasadena, California
December 1995

This report covers research conducted under a subcontract with the SAC Joint Venture which was funded by the Federal Emergency Management Agency (FEMA).

The SAC Joint Venture entered into a contract with the Federal Emergency Management Agency (FEMA) to furnish all professional, technical and clerical personnel, services, materials, equipment and facilities to conduct a "Program to Reduce Earthquake Hazards in Steel Moment Frame Structures." This publication reports on the research conducted under a subcontract between this Joint Venture and Professor Wilfred D. Iwan of the California Institute of Technology.

The SAC Joint Venture and the sponsoring agencies do not endorse any findings or conclusions. The Federal Emergency Management Agency and SAC Joint Venture are not responsible for any losses sustained as a result of the use of information or guidance contained in this publication.

Printing of Report EERL 95-07:

20 copies as follows:

- Xerox front-to-back

- NO printing on back of front cover

- Print cover on heavy blue stock (sample included)

- Special black-tape binding

Charge to account 31398

Send proof to Sharon Beckenbach, 104-44

Send printed copies to Philip Roche, 201 Thomas Building

Final Report on

Drift Demand Spectra for Selected Northridge Sites

by

Wilfred D. Iwan
California Institute of Technology

Submitted to
SAC Northridge Earthquake Project

Drift Demand Spectra For Selected Northridge Sites

Wilfred D. Iwan
CALIFORNIA INSTITUTE OF TECHNOLOGY

SUMMARY

This report presents uniformly processed data for ground motion at selected near-field sites where high peak velocities were observed during the Northridge earthquake. These data are used to produce drift demand spectra. Drift spectra are also presented for artificially generated Northridge ground motions. The results of the drift demand spectra are compared with results of numerical response evaluations of actual and prototype buildings.

Drift Demand Spectra for Selected Northridge Sites

INTRODUCTION

The objectives of this project were to: 1) provide uniformly processed data of ground motion at selected near-field (near-field source) sites where high peak ground velocities were observed during the Northridge earthquake, 2) produce drift demand spectra for selected near-field sites, 3) produce drift demand spectra for artificially generated Northridge ground motions provided by Paul Somerville, and 4) compare the results of the drift demand spectra to results of more extensive numerical analyses of prototype buildings subjected to the same ground motion.

The funding provided by SAC was, in itself, insufficient to achieve the above objectives. Therefore, the SAC funding was used to supplement funding received from NSF and other sources. The results of this project cannot be attributed to nor wholly owned by any sole sponsor.

NEAR-FIELD GROUND MOTION DATA

Table 2-1 shows the near-field stations that were examined under this project. Important properties of the measured ground motion at the selected sites are indicated in **Table 2-2**.

All accelerograph recordings for the stations indicated in **Table 2-1** were uniformly processed by the methods indicated in Iwan and Chen (1994). This includes appropriate instrument correction according to the instrument type, and baseline correction without band-pass filtering.

The time histories of the near-field ground motion for the uniformly processed data are reproduced in **Figures 2-1** through **2-16**. All data were rotated to N-S and E-W directions for uniformity. Shown in the figures are the acceleration, velocity, and displacement time histories. These time histories are available to researchers through e-mail and have been provided to all other SAC project teams upon request for use in their numerical analysis.

DRIFT DEMAND SPECTRA FOR RECORDED NORTHRIDGE DATA

Drift demand spectra were computed for each of the ground motion time histories generated above using the general approach described in Iwan (1994). These are reproduced in **Figures 2-17** through **2-24**.

It will be seen that the drift demand spectra have the general appearance of response spectra, but a close comparison will show that the detail shape of the drift demand spectra and response spectra is actually quite different. This difference is due to the fact that the two spectra contain essentially different information about the ground motion and its demand on a structure. For further discussion of this point, the reader is referred to in Iwan (1994).

DRIFT DEMAND SPECTRA FOR SYNTHETIC GROUND MOTIONS

As part of the SAC Northridge earthquake project, Dr. Paul Somerville generated several sets of synthetic ground motions to be used by other investigators in studies of building response. One set of data was generated for stations along a line running approximately north-northeast through the San Fernando Valley. This line is referred to as the Northridge Benchmark Profile. There are 21 stations along this profile. The largest horizontal ground acceleration was obtained at site 11 (herein referred to as NR11). The synthetic ground motion at this site was used by Professor John Hall in his building studies discussed later in this report. Hall rotated the ground motion data to determine the direction of maximum velocity change. His rotated data is used in this report.

Synthetic ground motions have also been generated for a postulated earthquake occurring on a buried thrust fault under downtown Los Angeles. One such set of simulated data was generated by T. Heaton and D. Wald. Station C05 of their data set was employed by Hall in his building studies. This data was also rotated to the direction of maximum velocity change.

Additional synthetic ground motions for an Elysian Park earthquake under downtown Los Angeles were generated by Somerville. Data for two stations (EP14 and EP17) were used by Hall in his building response studies. These ground motion time histories were also rotated to the direction of maximum velocity change.

The drift demand spectra for stations C05 and NR11 are shown in **Figure 2-25**. The drift demand spectra for stations EP14 and EP17 are shown in **Figure 2-26**.

From **Figure 2-25**, it is seen that the drift demand spectrum of the NR11 synthetic ground motion is substantially higher than that of any of the measured Northridge ground motions. The synthetic EP ground motions in **Figures 2-27 through 2-29** also possess a drift demand spectrum that exceeds the spectrum of measured Northridge ground motions, particularly in the range of 1.5-2.5 sec period. Whether such high drift demand will be measured in real earthquakes remains to be seen. However, the drift demand spectra for these synthetic ground motions are useful in indicating potentially very high drift demand associated with near field earthquakes. Such demand can not be ignored in structural design.

Somerville has also generated synthetic Northridge ground motions for a number of sites where damaged buildings were located. Three sites, referred to as Sites 01-03 or the Canoga sites, were sufficiently close together that only one set of ground motion time histories was generated for the three sites. The synthetic ground motion was generated on a grid of nine points with a 1 km spacing surrounding the center station. The N-S direction synthetic ground motions were used by Professor Gary Hart to study the performance of certain damaged buildings in this area. The drift demand spectra for the synthetic ground motions in the N-S direction at nine grid points is given in **Figures 2-27 through 2-29**.

COMPARISON WITH DETAILED STRUCTURAL RESPONSE CALCULATIONS BY HALL

Professor Hall performed detailed numerical studies of prototype 20-story and 6-story buildings subjected to measured Northridge ground motions and synthetic Northridge and Elysian Park ground motions. The computed ground floor drift ratios are given in **Tables 2-3** and **2-4**. Comparing the results of the tables with **Figures 2-21, 2-25, and 2-27**, it is observed that the results of the drift demand spectra agree very well with the results of Hall's detailed elastic building model studies. Indeed, the drift demand spectra results for the 2% and 10% spectra usually bound Hall's elastic results. It is concluded that the linear drift demand spectrum gives a good indication of drift demand even for fairly complex elastic building structures.

The drift results generated by Hall from his plastic model are sometimes substantially higher than those for the elastic model. This is particularly true for the shorter building with a linear period of 1.36 sec.

One possible explanation for the increase in drift ratio is an effective increase in the period of the structure. This has *two* effects on the drift demand spectrum. First, the wavespeed within the structure is decreased. This causes a direct increase in drift ratio in proportion to the increase in period. Additionally, the drift demand spectrum will be effectively shifted to the left by an amount equal to the overall period shift. These effects, taken together, can explain the higher drift ratios computed by Hall for his plastic building model.

As a first attempt to generate a ductility-based drift demand spectrum, the empirical effective period relationship employed by Iwan (1980) for a family of hysteretic systems was used to adjust the linear drift demand spectra for the NR11 and C05 records. The results are shown in **Figure 2-30**. It is observed that the ductility-based drift demand spectrum results agree well with the results of Hall's detailed plastic building model computations. This is further confirmation of the usefulness of the drift demand spectrum concept.

For the cases in which bad joints are included by Hall, many of the building models collapsed. This might be a direct consequence of the very high drift ratios that already exist in the plastic (but undamaged) models. It is also likely a consequence of even further softening of the buildings through the joint failure mechanism. From the ductility-based drift demand spectra of **Figure 2-30**, it is seen that the period lengthening effect will have the greatest effect on drift demand for the *shorter* period building (1.36 sec) as the slope of the spectra are greatest at this period. Hence, from the drift demand spectra, one would expect a greater likelihood of collapse for the shorter period building when bad joints are included. Indeed, this is just what is observed in Hall's study. This, there is further confirmation of the usefulness of the drift demand spectrum.

COMPARISON WITH DETAILED STRUCTURAL RESPONSE CALCULATIONS BY HART

Professor Hart studied the response of a computer model of a 6-story building subjected to the grid of synthetic ground motions generated by Somerville for Stations 01-03. His ground floor drift results are summarized in **Table 2-5**. A comparison of the results in **Table 2-5** and **Figures 2-23** and **2-27** through **2-29** indicates fairly close agreement between the drift demand spectrum results and those of the detailed numerical computation. If anything, the linear drift demand spectra are slightly conservative compared to the detailed numerical computation results.

If period lengthening due to yielding is taken into account, the building studies by Hart lie near a *trough* of the drift demand spectra for this site. Based on the drift demand spectra, taller buildings near this site with effective periods in the range of 1.5-2.2 sec might be expected to have experienced considerably higher drift demand than the 6-story building that was modeled. The drift demand spectra indicate that the drift could have been of the order of 2% for such structures. Studies by other SAC investigators of taller buildings near the same site seem to confirm higher ductility ratios than those obtained for the 6-story building investigated by Hart. However, further study of this point is needed.

CONCLUSIONS

Based on the results of this limited study, it is concluded that the drift demand spectrum has promise as a simple means of describing drift demand for real structures subjected to damaging earthquakes. For buildings in the elastic range, good agreement is obtained between the simple drift demand spectrum and detailed numerical computations. For buildings that are strongly nonlinear, some adjustment needs to be made to the drift demand spectrum just as in the case of the response spectrum. A simple period adjustment seems to work well for the limited number of cases considered in this study. Further efforts to develop ductility-based drift demand spectra are currently underway.

TABLE 2-1: SELECTED NEAR-FIELD GROUND ACCELEROGRAMS
FROM THE NORTHRIDGE EARTHQUAKE

Station Name	Code	Epic. Dist. (km)	Soil Condition	Type Instr.	Owner
Arleta Fire Stn.	ARL	9		SMA-1	CDMG
Rinaldi Receiving Stn.	RRS	10	Alluvium	SMA-1	LADWP
Sylmar Conver Stn.	SCS	12	Alluvium	CRA-1	LADWP
Sylmar Conv. Stn.-East	CSE	13	Sed. Rock	SMA-1	LADWP
Sylmar Co. Hospital	SCH	16	Alluvium	SMA-1	CDMG
Newhall Co. Fire Stn.	NHL	19		SMA-1	CDMG
Pardee Stn.	PAR	24		SMA-2	SCE
Santa Monica City Hall	SAN	24	Alluvium	SMA-1	CDMG

Drift Demand Spectra for Selected Northridge Sites

TABLE 2-2: PEAK ACCELERATION, VELOCITY AND DISPLACEMENT FOR
SELECTED ACCELEROGRAMS.

Station	Direction	PGA (g)	PGV (cm/s)	PGD (cm)
ARL	N-S	0.30	-24	-16
	E-W	0.34	-39	17
RRS	N-S	0.82	-159	-59
	E-W	0.57	102	-74
SCS	N-S	0.78	-134	43
	E-W	0.57	-77	45
CSE	N-S	0.75	-112	-30
	E-W	0.47	-67	41
SCH	N-S	0.88	-136	-48
	E-W	0.63	-81	-31
NHL	N-S	0.59	-98	39
	E-W	-0.60	-75	22
PAR	N-S	-0.49	-60	-18
	E-W	-0.31	46	-42
SMC	N-S	-0.40	27	-13
	E-W	-0.87	41	-17
ELC (ref)	N-S	0.35	33	11

TABLE 2-3: GROUND FLOOR DRIFT RATIO COMPUTED BY HALL FROM DETAILED
MODELING OF PROTOTYPE TWENTY STORY BUILDING WITH LINEAR
FUNDAMENTAL PERIOD OF 3.5 SEC.

Earthquake Excitation	Type Model	Computed Drift (%)
SCH (N-S)	Elastic	1.0
SCH (N-S)	Plastic	1.4
SCH (N-S)	Bad Joints	1.3
CO5 (MAX)	Elastic	2.1
CO5 (MAX)	Plastic	3.7
CO5 (MAX)	Bad Joints	Collapse
NR11 (MAX)	Elastic	1.5
NR11 (MAX)	Plastic	2.4
NR11 (MAX)	Bad Joints	2.4
EP14 (MAX)	Elastic	2.1
EP14 (MAX)	Plastic	4.2
EP14 (MAX)	Bad Joints	5.7-Collapse

Drift Demand Spectra for Selected Northridge Sites

TABLE 2-4: GROUND FLOOR DRIFT RATIO COMPUTED BY HALL FROM DETAILED MODELING OF PROTOTYPE SIX STORY BUILDING WITH LINEAR FUNDAMENTAL PERIOD OF 1.36 SEC.

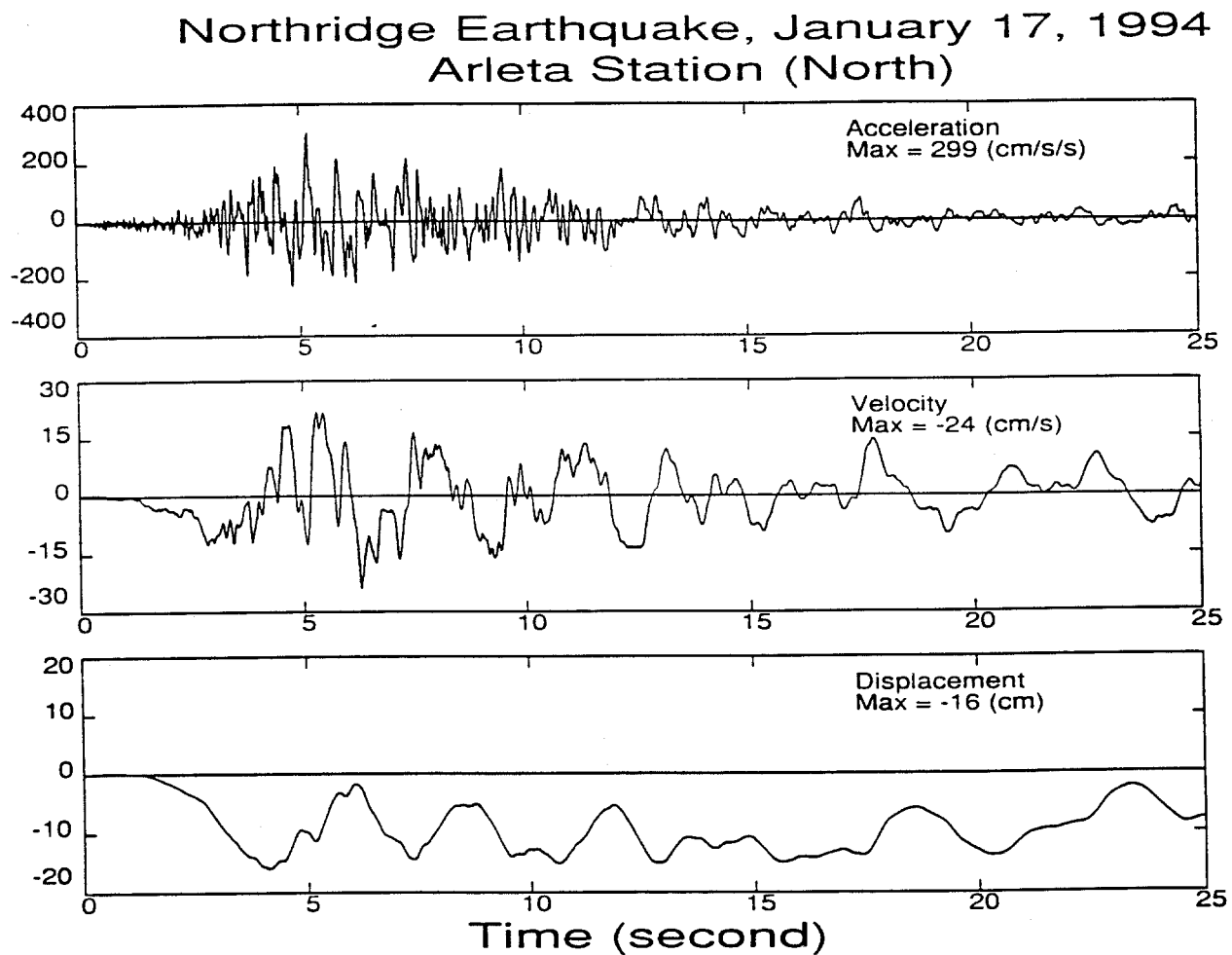
Earthquake Excitation	Type Model	Computed Drift (%)
SCH (N-S)	Elastic	2.6
SCH (N-S)	Plastic	2.7
SCH (N-S)	Bad Joints	Collapse
CO5 (MAX)	Elastic	1.8
CO5 (MAX)	Plastic	7.9
CO5 (MAX)	Bad Joints	14.7-Collapse
NR11 (MAX)	Elastic	4.6
NR11 (MAX)	Plastic	6.7
NR11 (MAX)	Bad Joints	Collapse
EP17 (MAX)	Elastic	3.8
EP17 (MAX)	Plastic	7.3
EP17 (MAX)	Bad Joints	5.5-Collapse

TABLE 2-5: GROUND FLOOR DRIFT RATIO COMPUTED BY HART FROM DETAILED MODELING OF A SIX STORY BUILDING WITH LINEAR FUNDAMENTAL PERIOD OF 0.82 SEC SUBJECTED TO GRID OF NORTHRIDGE GROUND MOTIONS GENERATED BY SOMMERVILLE.

Earthquake Excitation	Computed Drift (%)
NRGRD 01-03, NW (N-S)	0.7
NRGRD 01-03, N (N-S)	1.1
NRGRD 01-03, NE (N-S)	0.9
NRGRD 01-03, W (N-S)	1.0
NRGRD 01-03, C (N-S)	0.8
NRGRD 01-03, E (N-S)	0.9
NRGRD 01-03, SW (N-S)	0.9
NRGRD 01-03, S (N-S)	1.1
NRGRD 01-03, SE (N-S)	0.8
PAR (N-S)	1.2

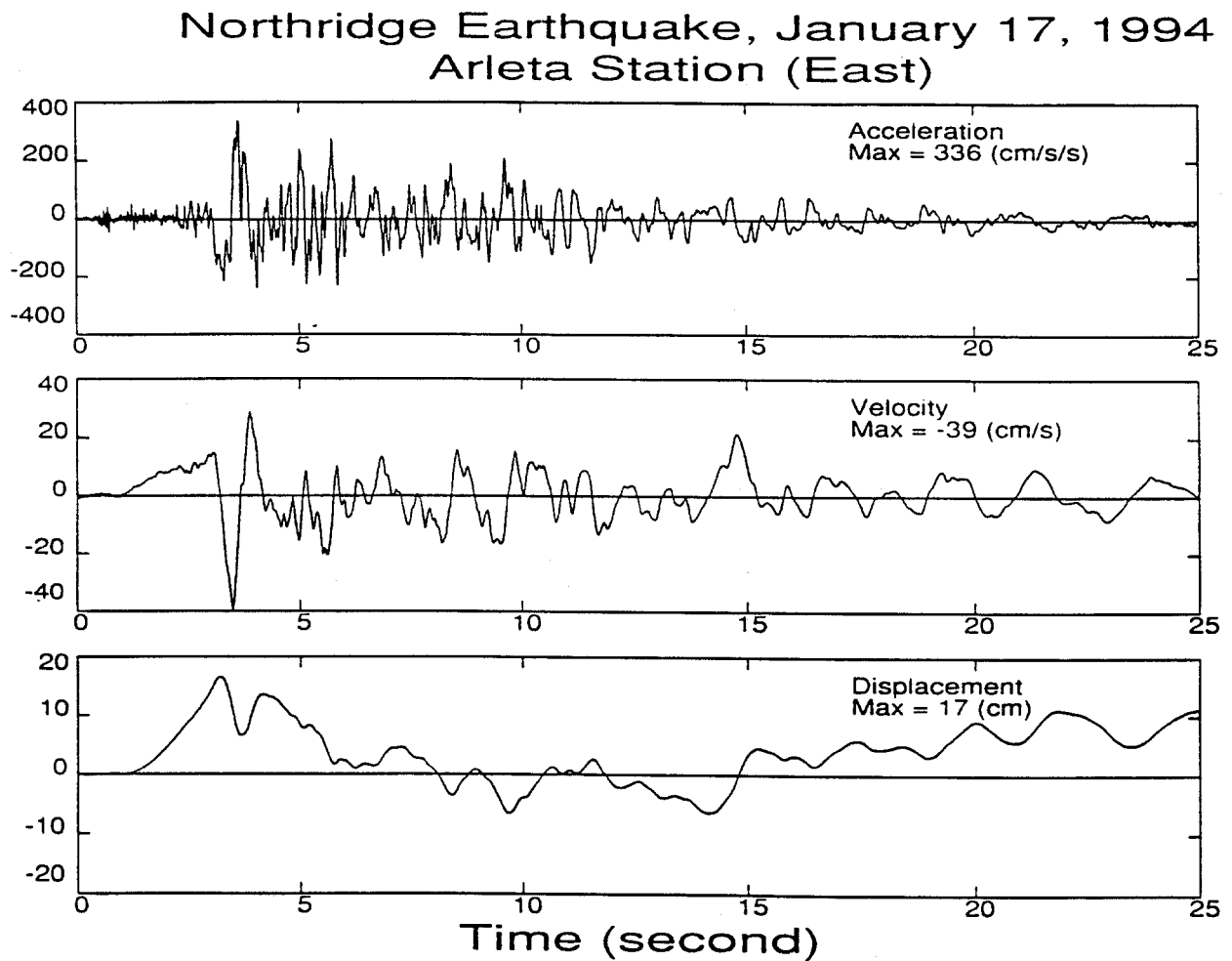
Drift Demand Spectra for Selected Northridge Sites

FIGURE 2-1: ACCELERATION, VELOCITY AND DISPLACEMENT TIME HISTORIES.
ARL, N-S



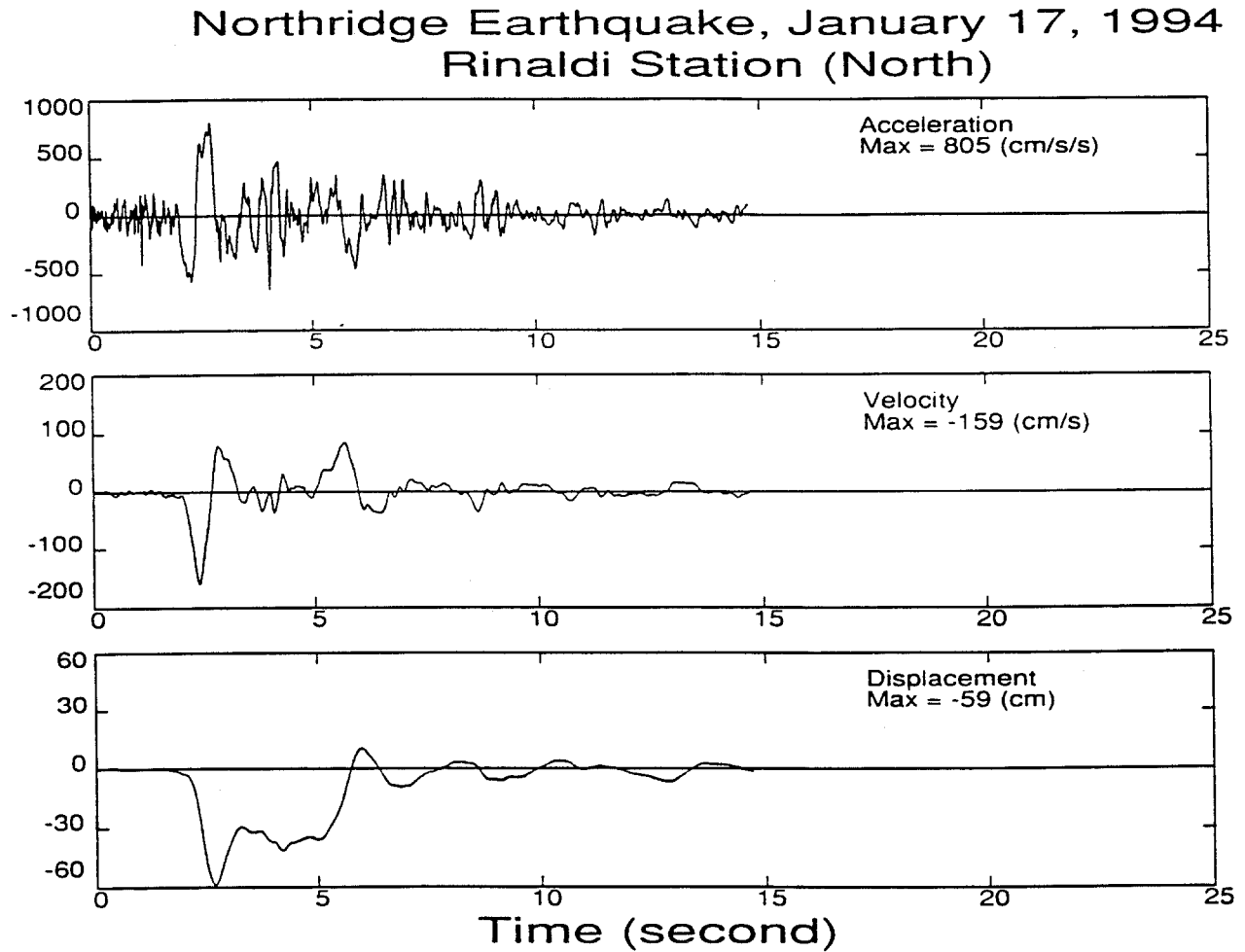
Drift Demand Spectra for Selected Northridge Sites

FIGURE 2-2: ACCELERATION, VELOCITY AND DISPLACEMENT TIME HISTORIES.
ARL, E-W



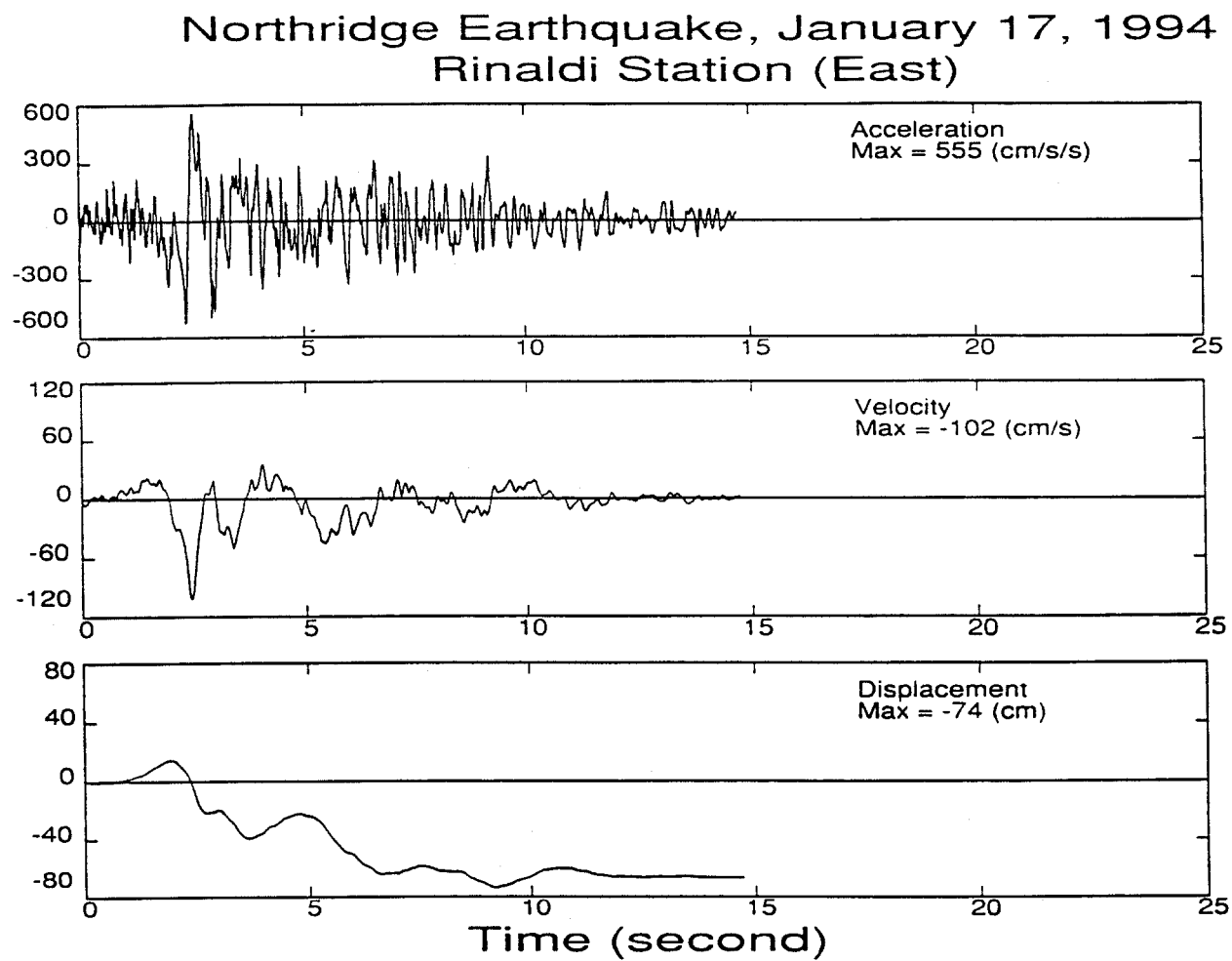
Drift Demand Spectra for Selected Northridge Sites

FIGURE 2-3: ACCELERATION, VELOCITY AND DISPLACEMENT TIME HISTORIES.
RRS, N-S



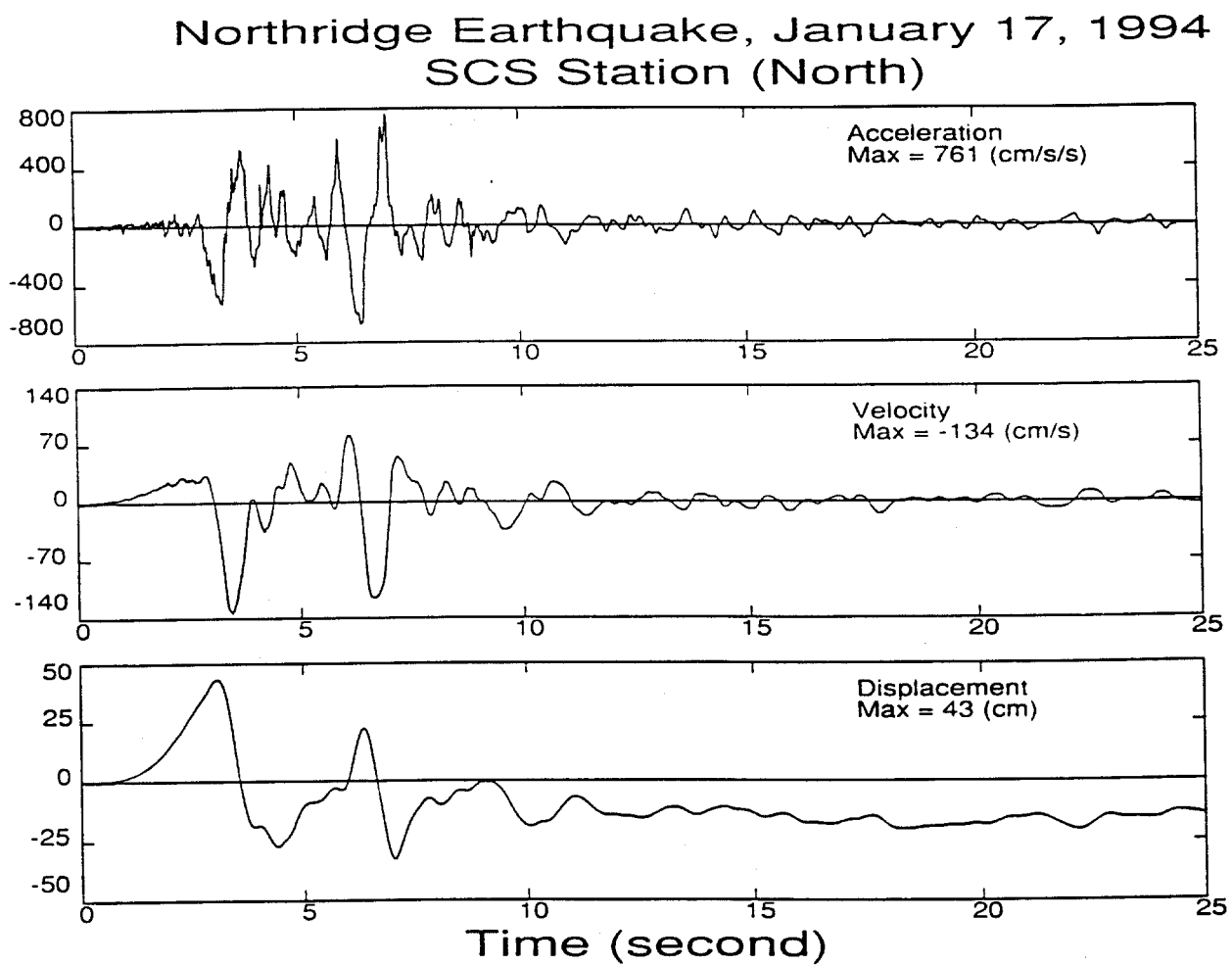
Drift Demand Spectra for Selected Northridge Sites

FIGURE 2-4: ACCELERATION, VELOCITY AND DISPLACEMENT TIME HISTORIES.
RRS, E-W



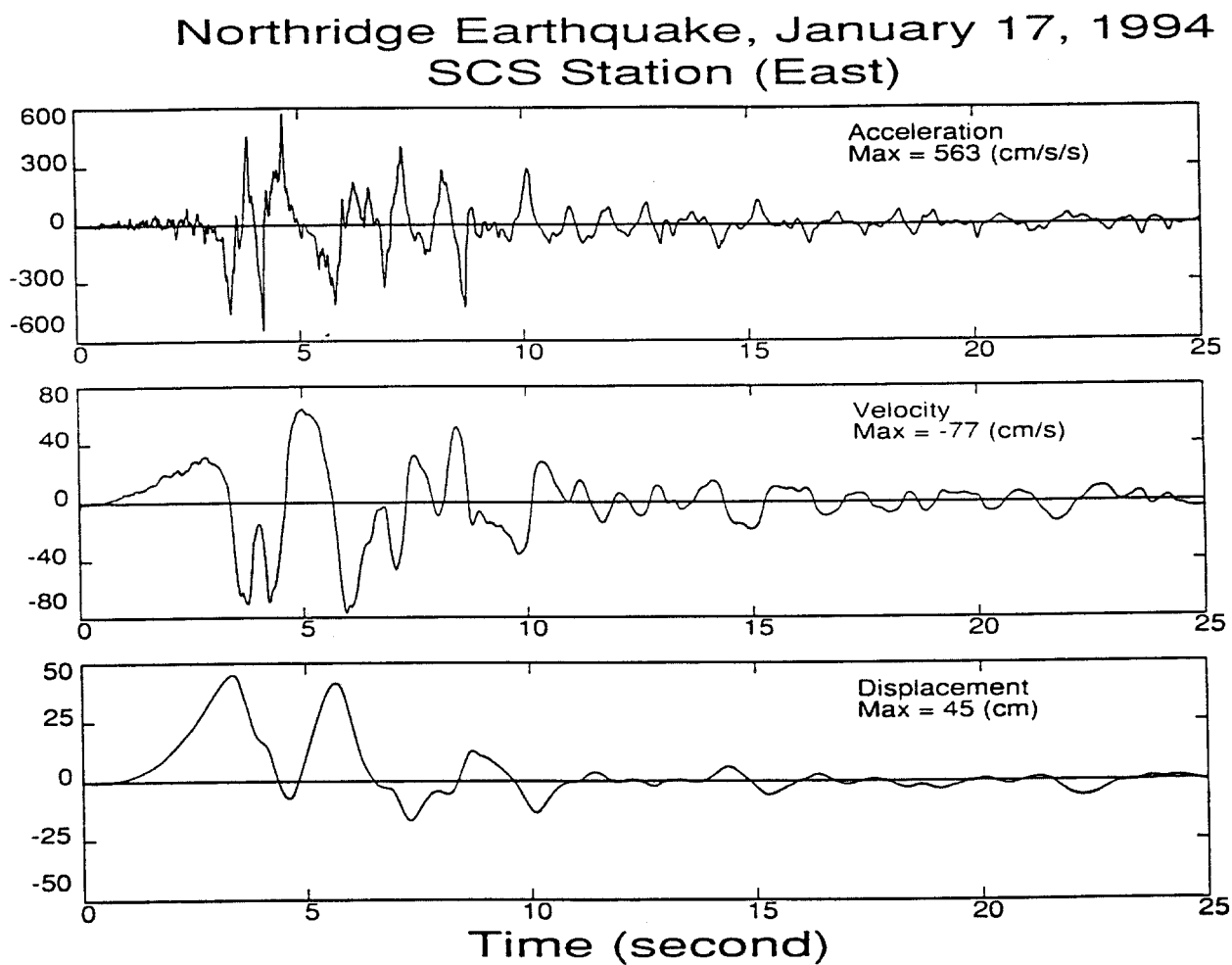
Drift Demand Spectra for Selected Northridge Sites

FIGURE 2-5: ACCELERATION, VELOCITY AND DISPLACEMENT TIME HISTORIES.
SCS, N-S



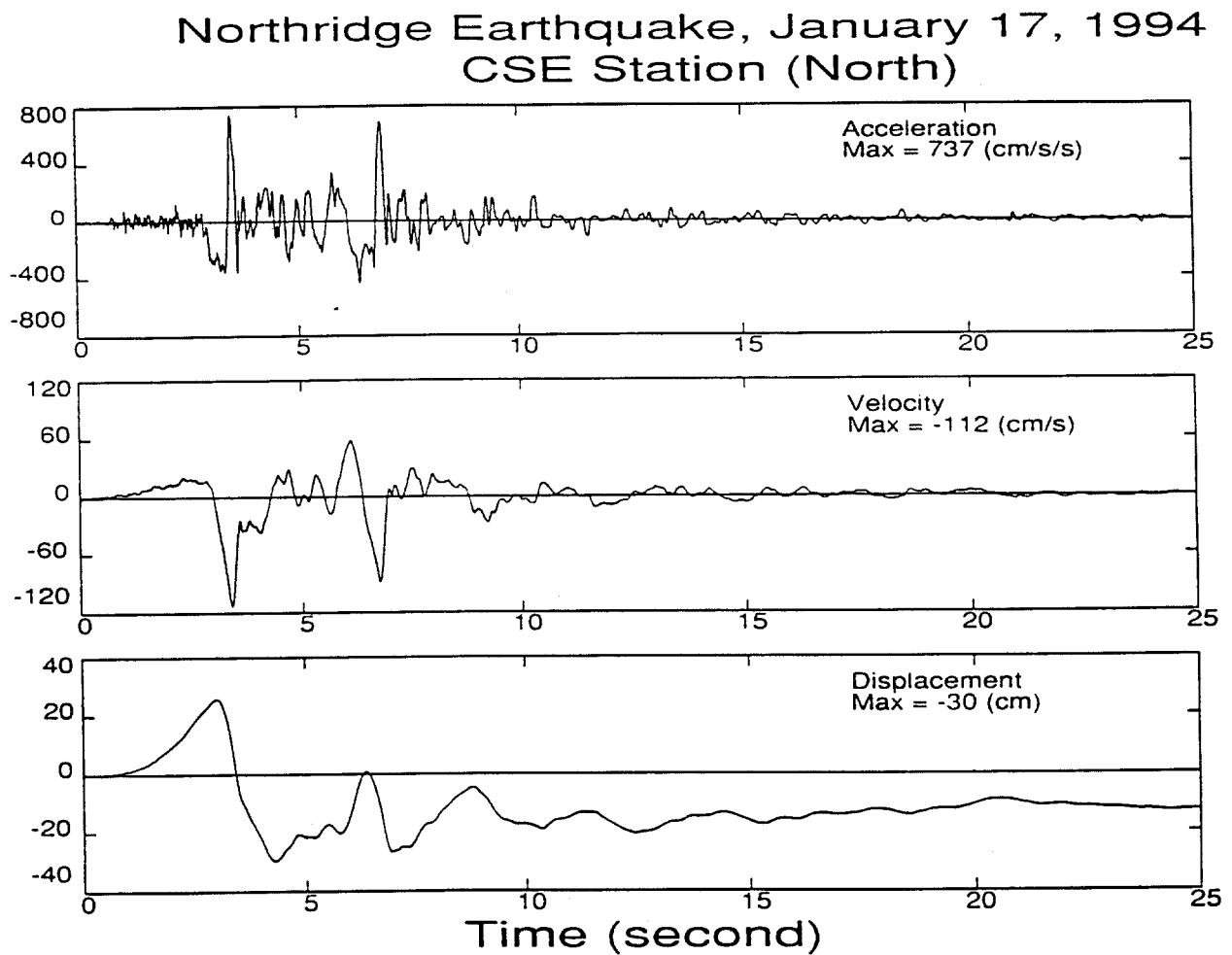
Drift Demand Spectra for Selected Northridge Sites

FIGURE 2-6: ACCELERATION, VELOCITY AND DISPLACEMENT TIME HISTORIES.
SCS, E-W



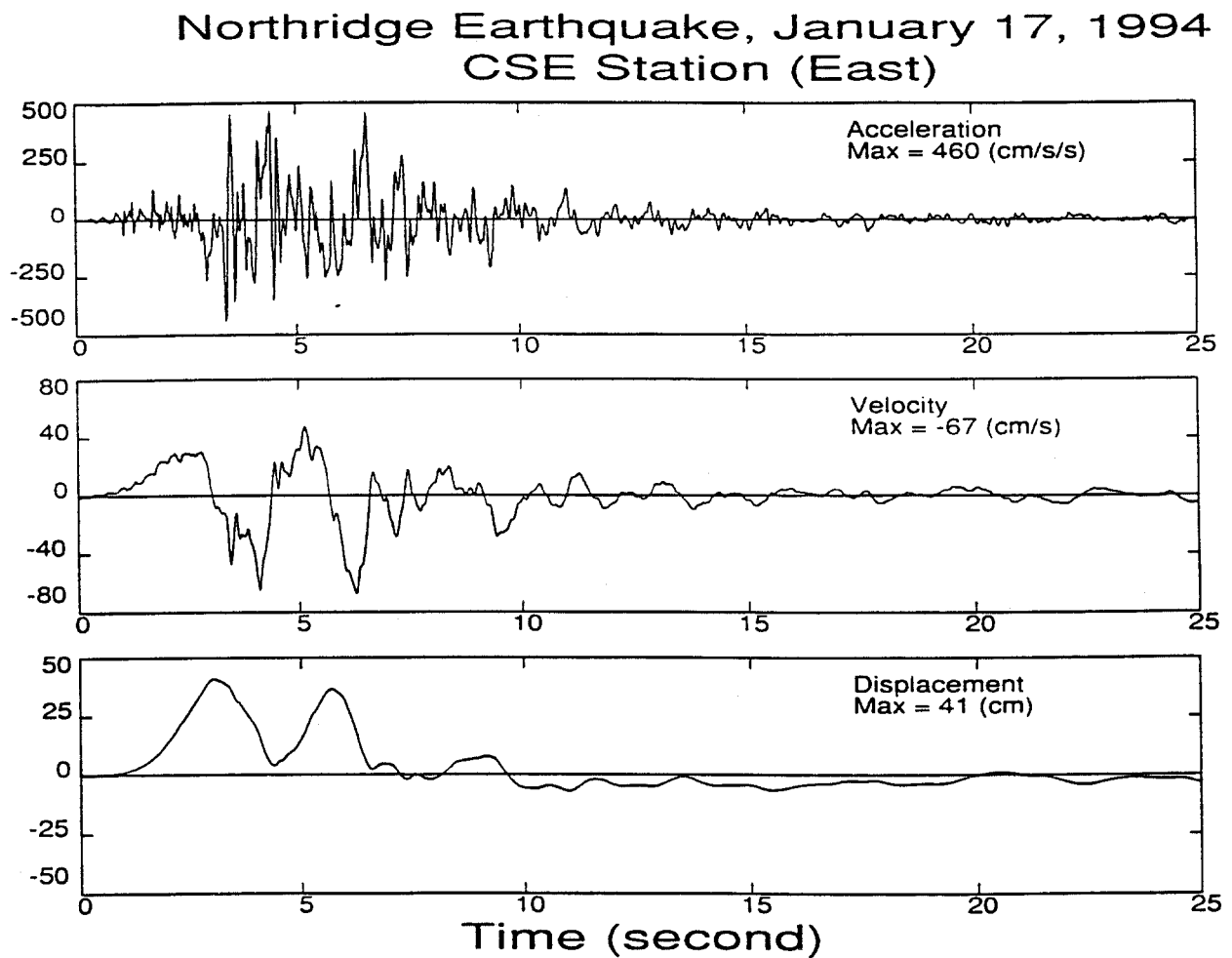
Drift Demand Spectra for Selected Northridge Sites

FIGURE 2-7: ACCELERATION, VELOCITY AND DISPLACEMENT TIME HISTORIES.
CSE, N-S



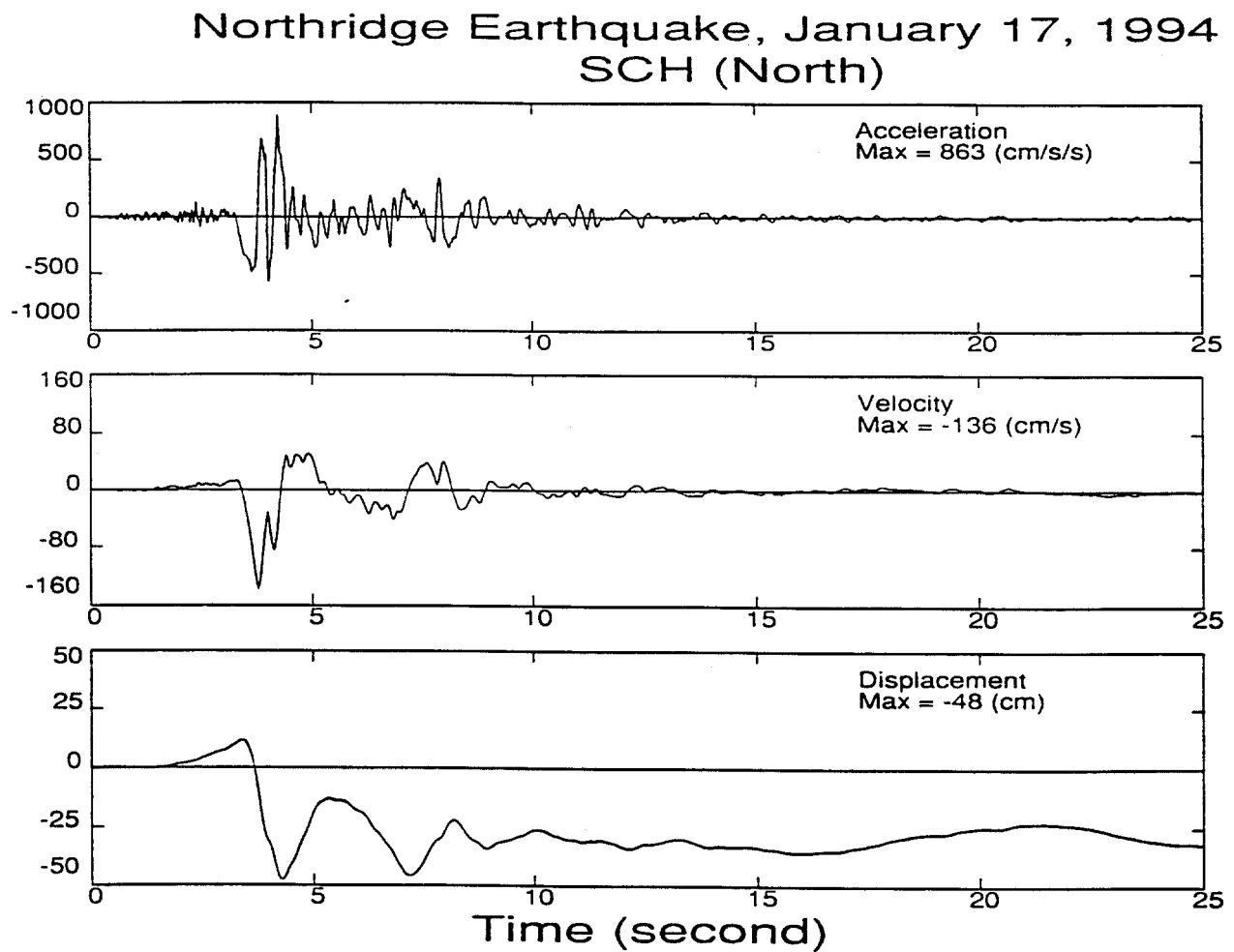
Drift Demand Spectra for Selected Northridge Sites

FIGURE 2-8: ACCELERATION, VELOCITY AND DISPLACEMENT TIME HISTORIES.
CSE, E-W



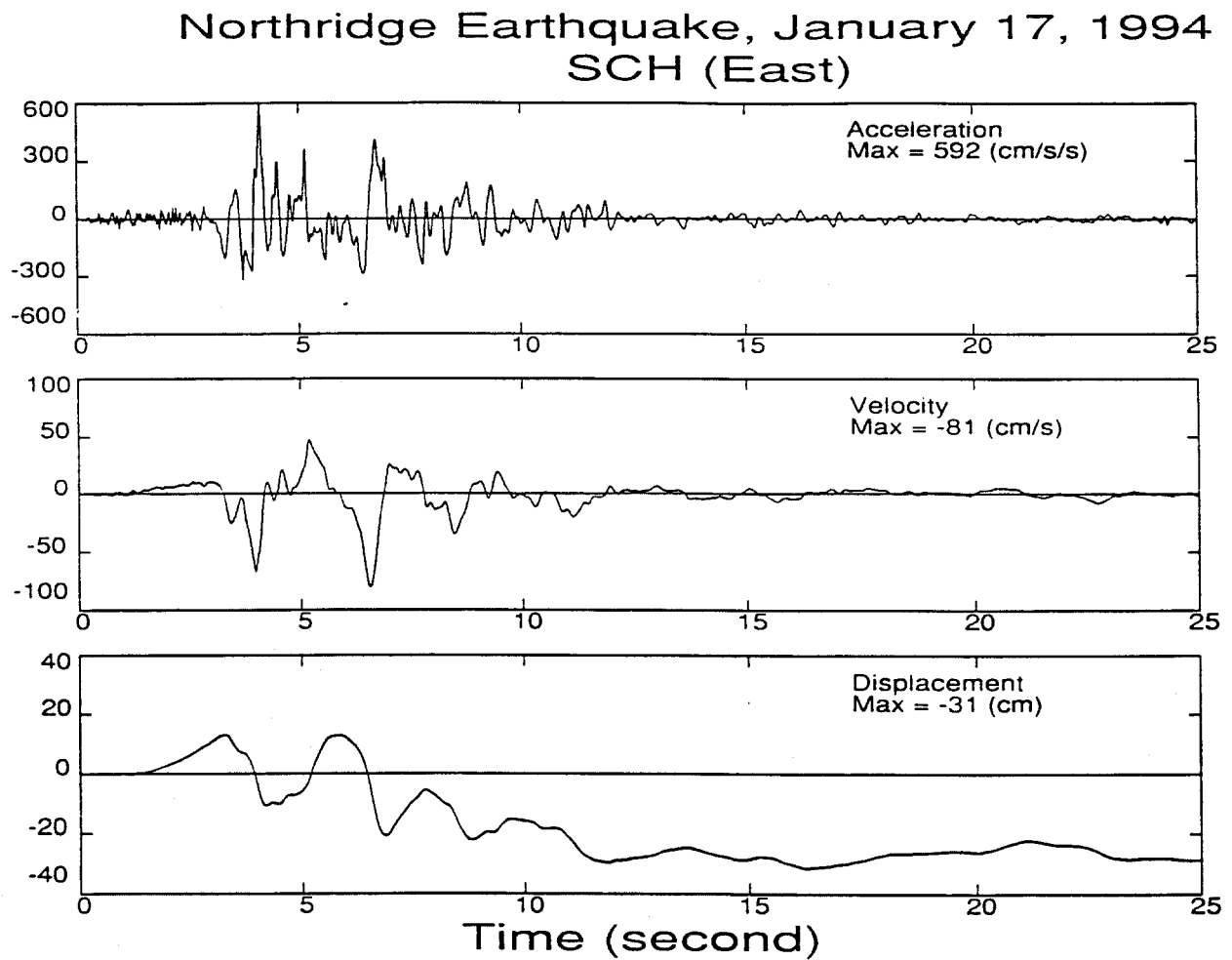
Drift Demand Spectra for Selected Northridge Sites

FIGURE 2-9: ACCELERATION, VELOCITY AND DISPLACEMENT TIME HISTORIES.
SCH, N-S



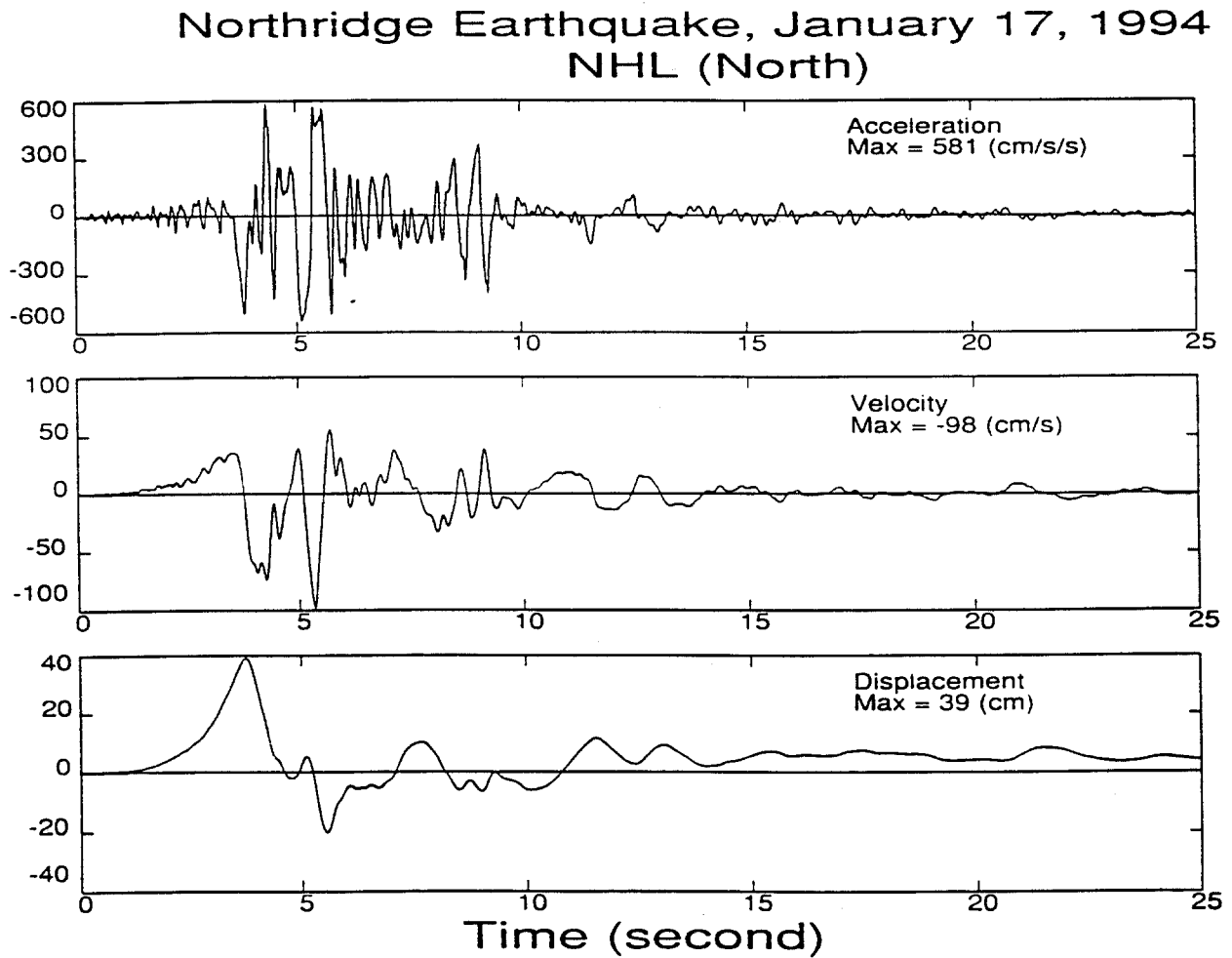
Drift Demand Spectra for Selected Northridge Sites

FIGURE 2-10: ACCELERATION, VELOCITY AND DISPLACEMENT TIME HISTORIES.
SCH, E-W



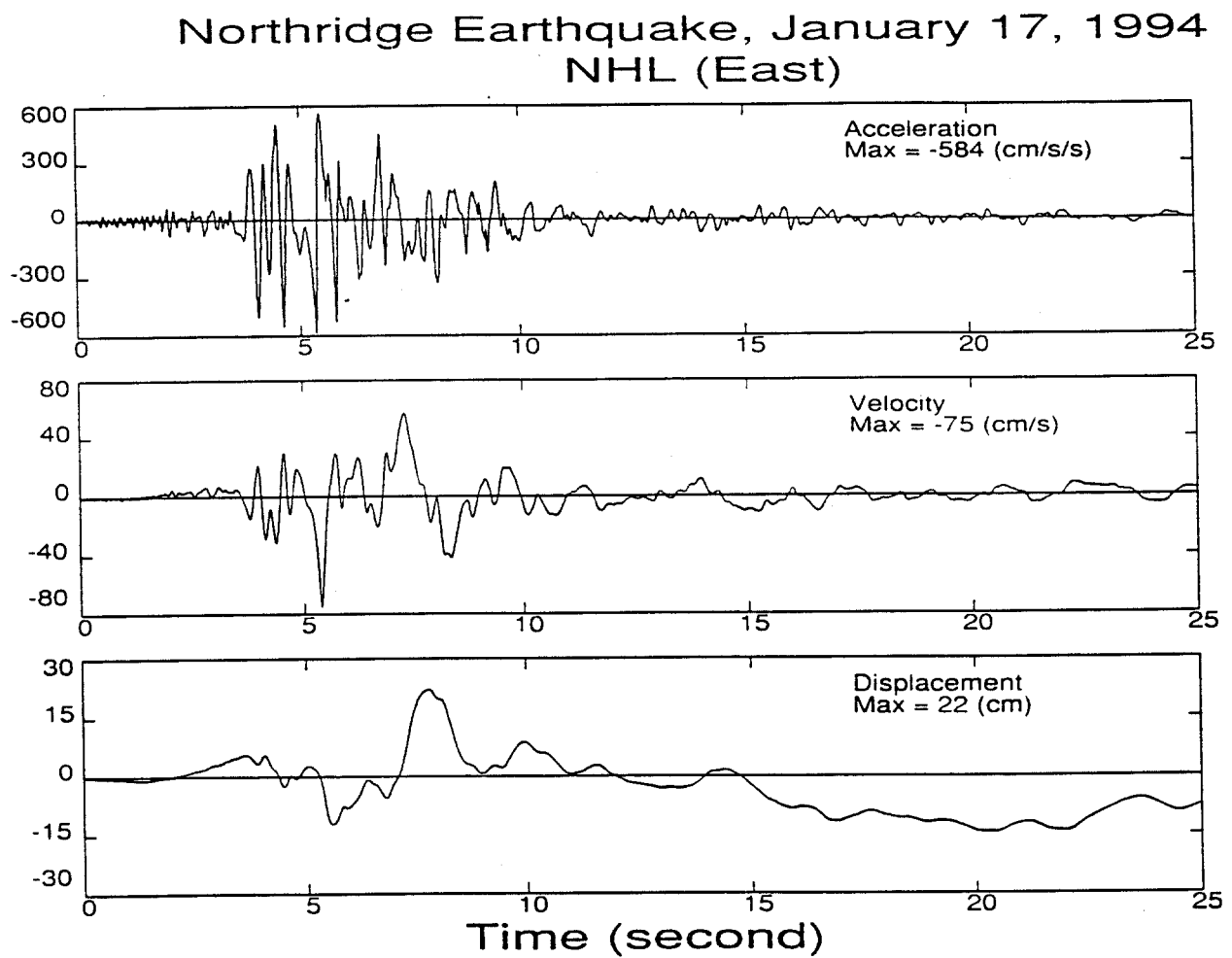
Drift Demand Spectra for Selected Northridge Sites

FIGURE 2-11: ACCELERATION, VELOCITY AND DISPLACEMENT TIME HISTORIES.
NHL, N-S



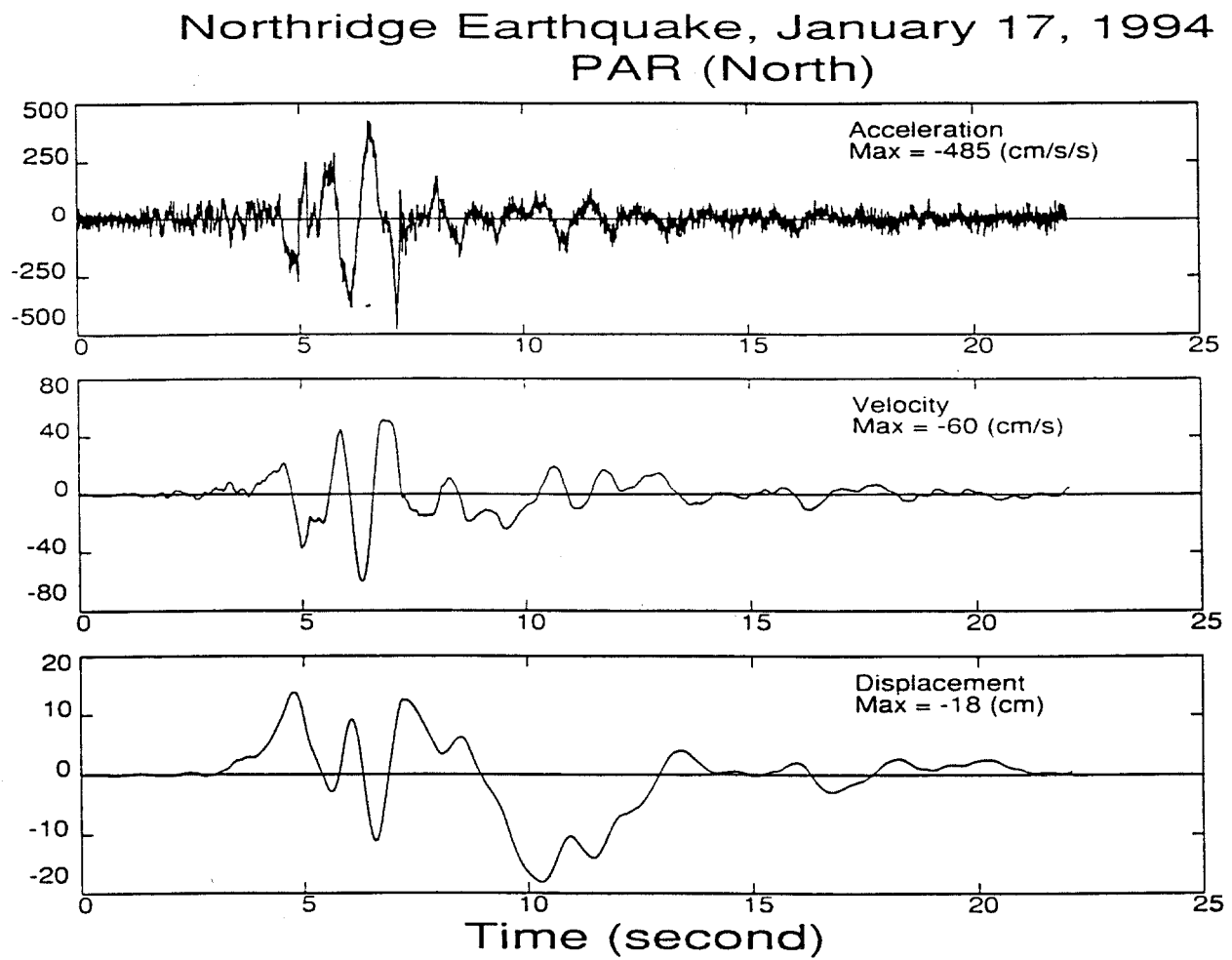
Drift Demand Spectra for Selected Northridge Sites

FIGURE 2-12: ACCELERATION, VELOCITY AND DISPLACEMENT TIME HISTORIES.
NHL, E-W



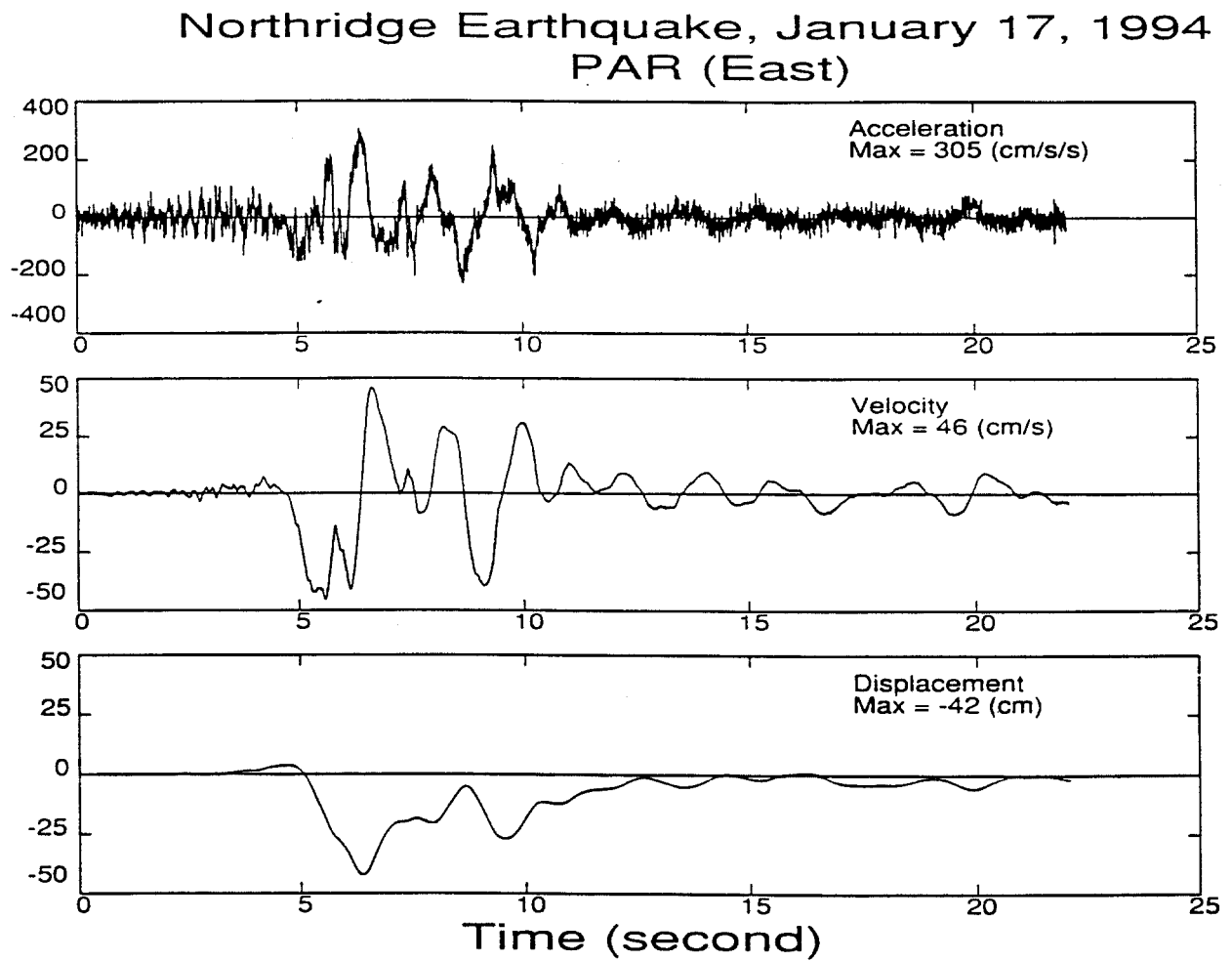
Drift Demand Spectra for Selected Northridge Sites

FIGURE 2-13: ACCELERATION, VELOCITY AND DISPLACEMENT TIME HISTORIES.
PAR, N-S



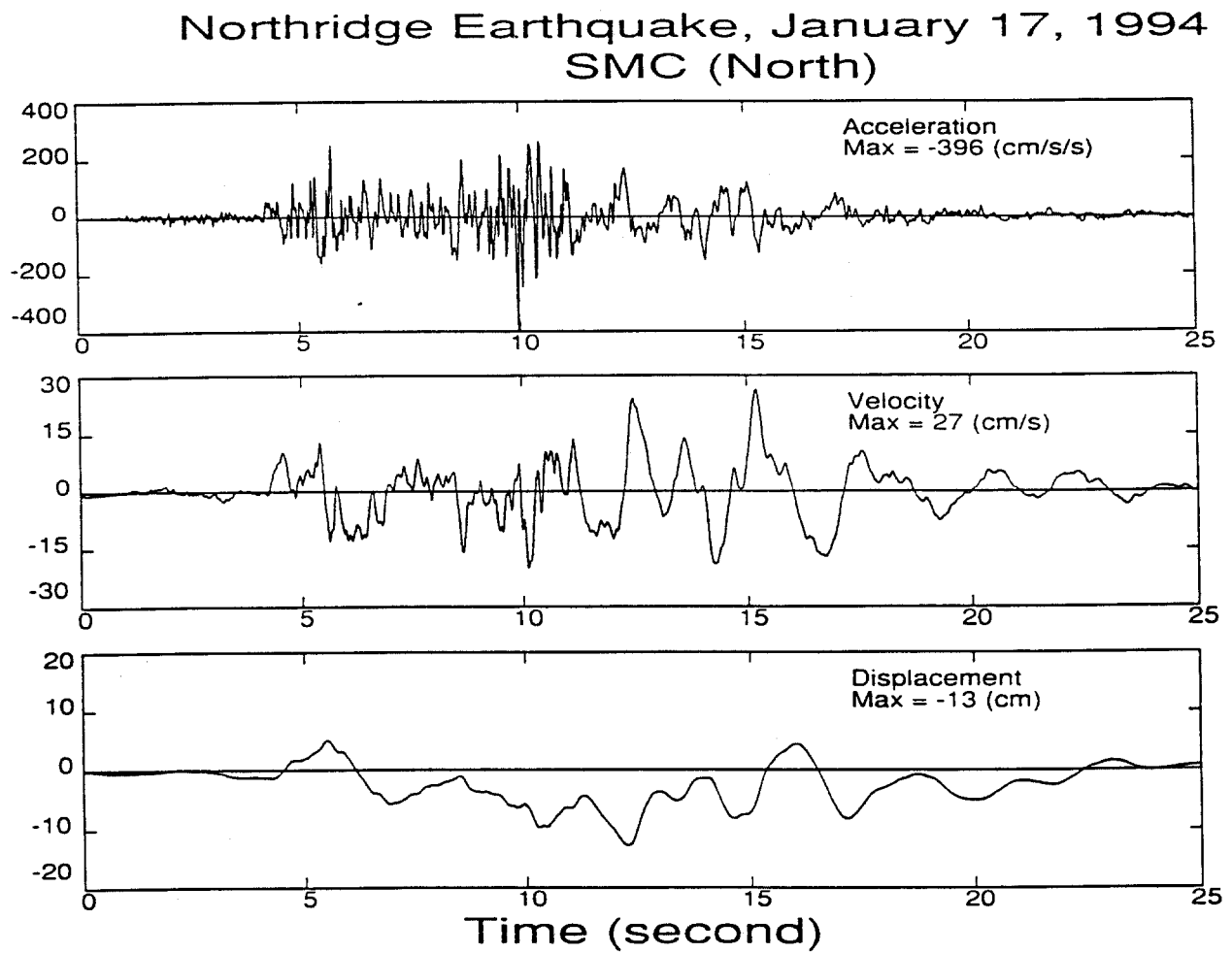
Drift Demand Spectra for Selected Northridge Sites

FIGURE 2-14: ACCELERATION, VELOCITY AND DISPLACEMENT TIME HISTORIES.
PAR, E-W



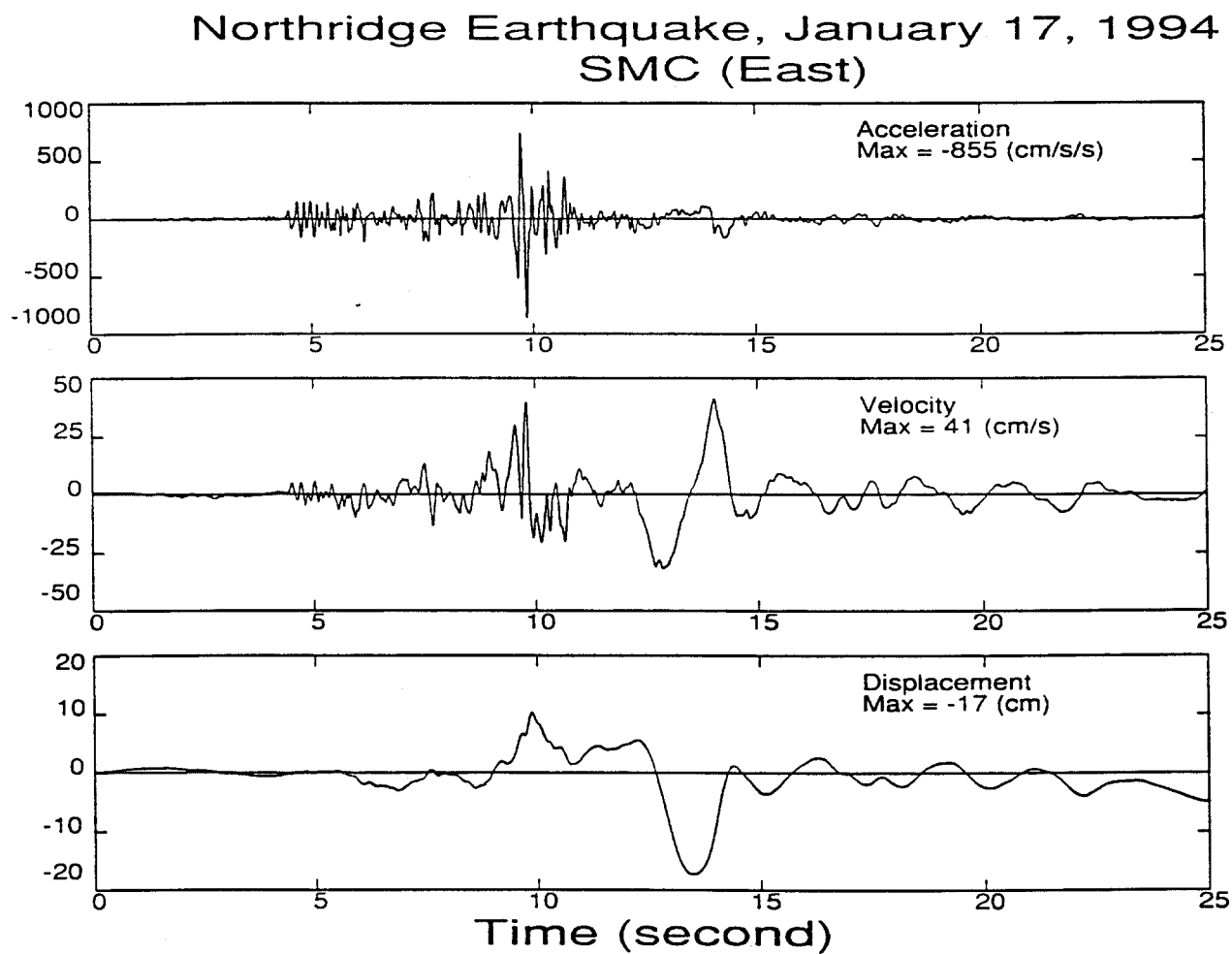
Drift Demand Spectra for Selected Northridge Sites

FIGURE 2-15: ACCELERATION, VELOCITY AND DISPLACEMENT TIME HISTORIES.
SMC, N-S



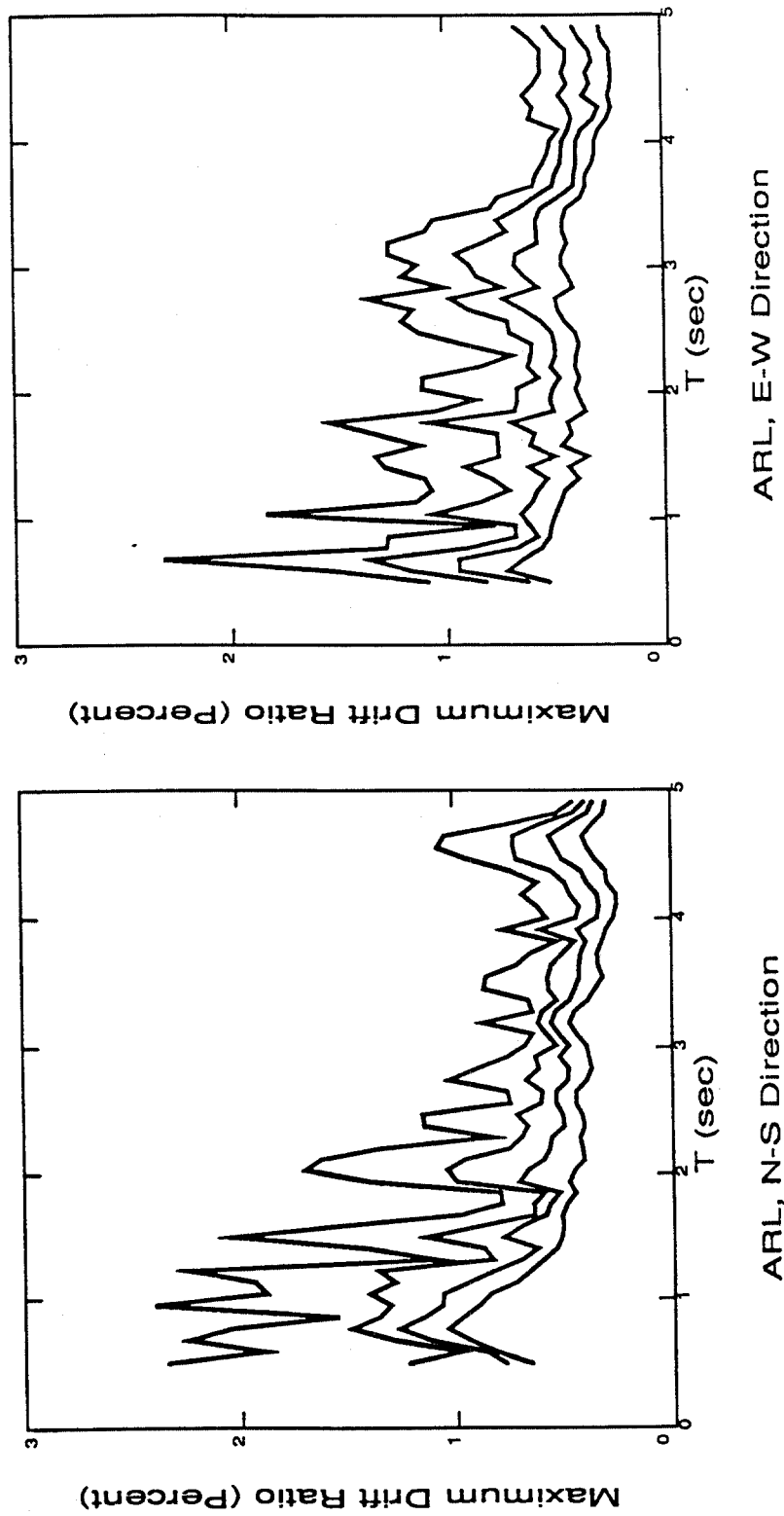
Drift Demand Spectra for Selected Northridge Sites

FIGURE 2-16: ACCELERATION, VELOCITY AND DISPLACEMENT TIME HISTORIES.
SMC, E-W



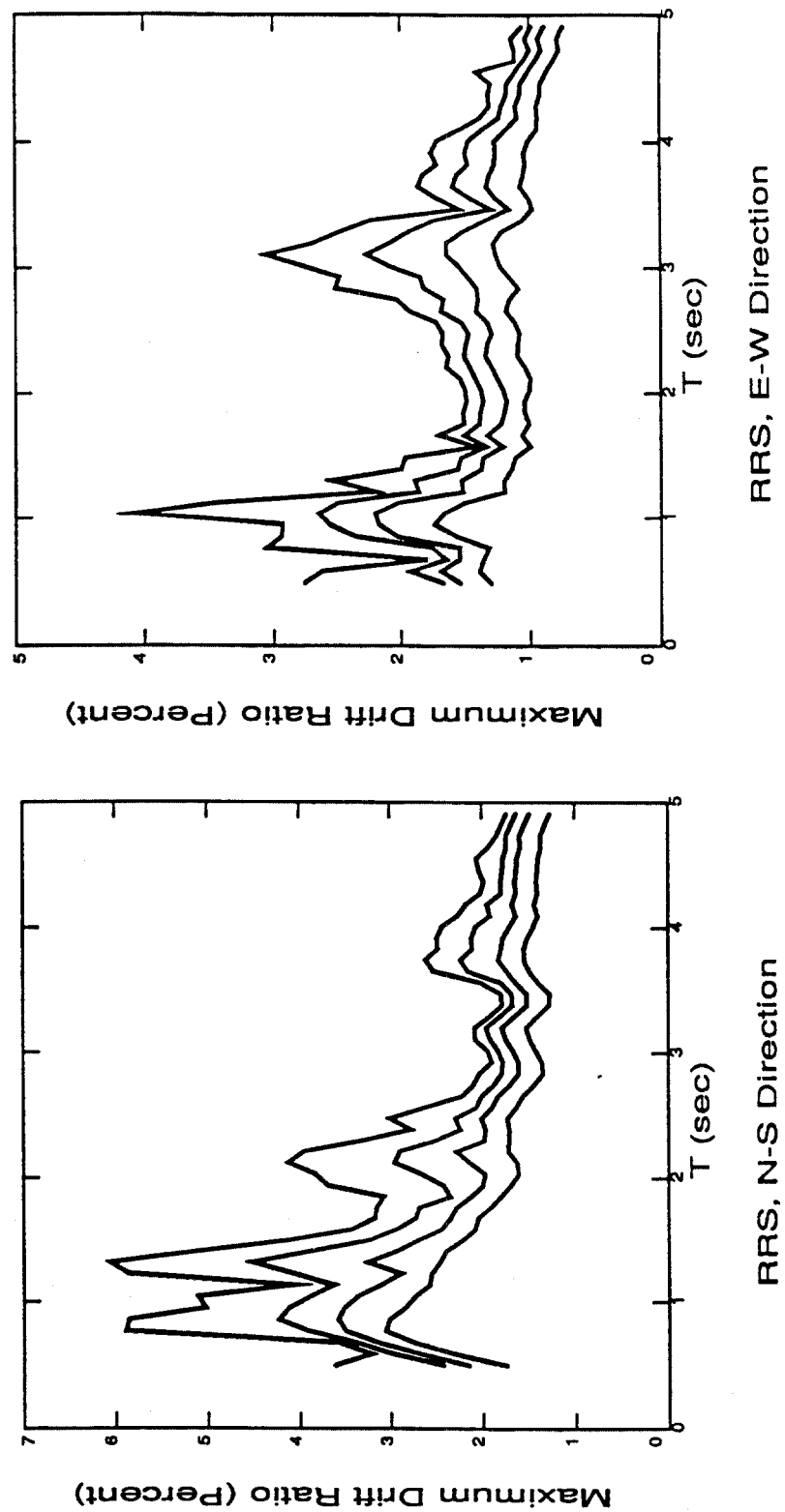
Drift Demand Spectra for Selected Northridge Sites

FIGURE 2-17: DRIFT DEMAND SPECTRA. 0, 2, 5, AND 10% DAMPING. ARL



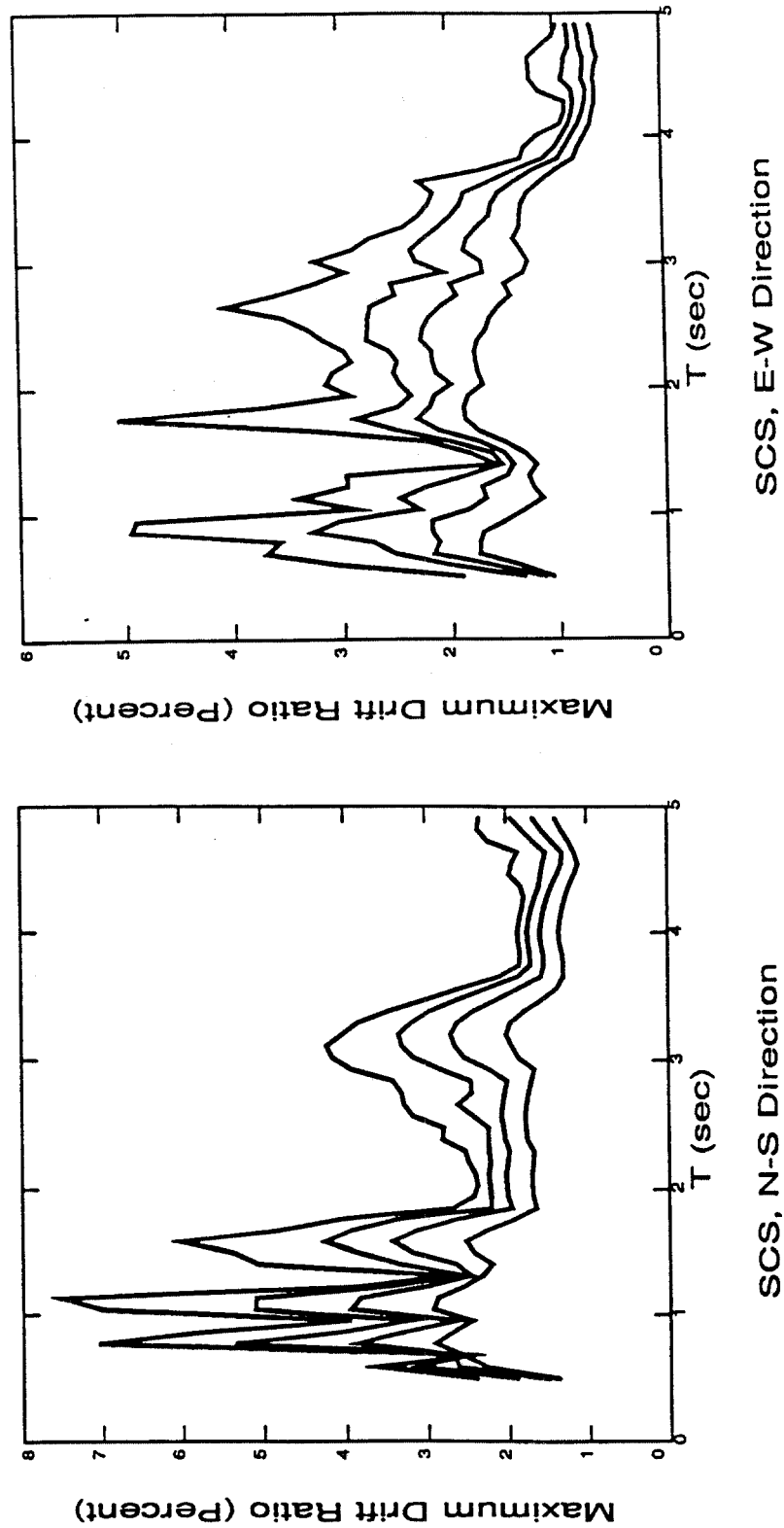
Drift Demand Spectra for Selected Northridge Sites

FIGURE 2-18: DRIFT DEMAND SPECTRA. 0, 2, 5, AND 10% DAMPING. RRS



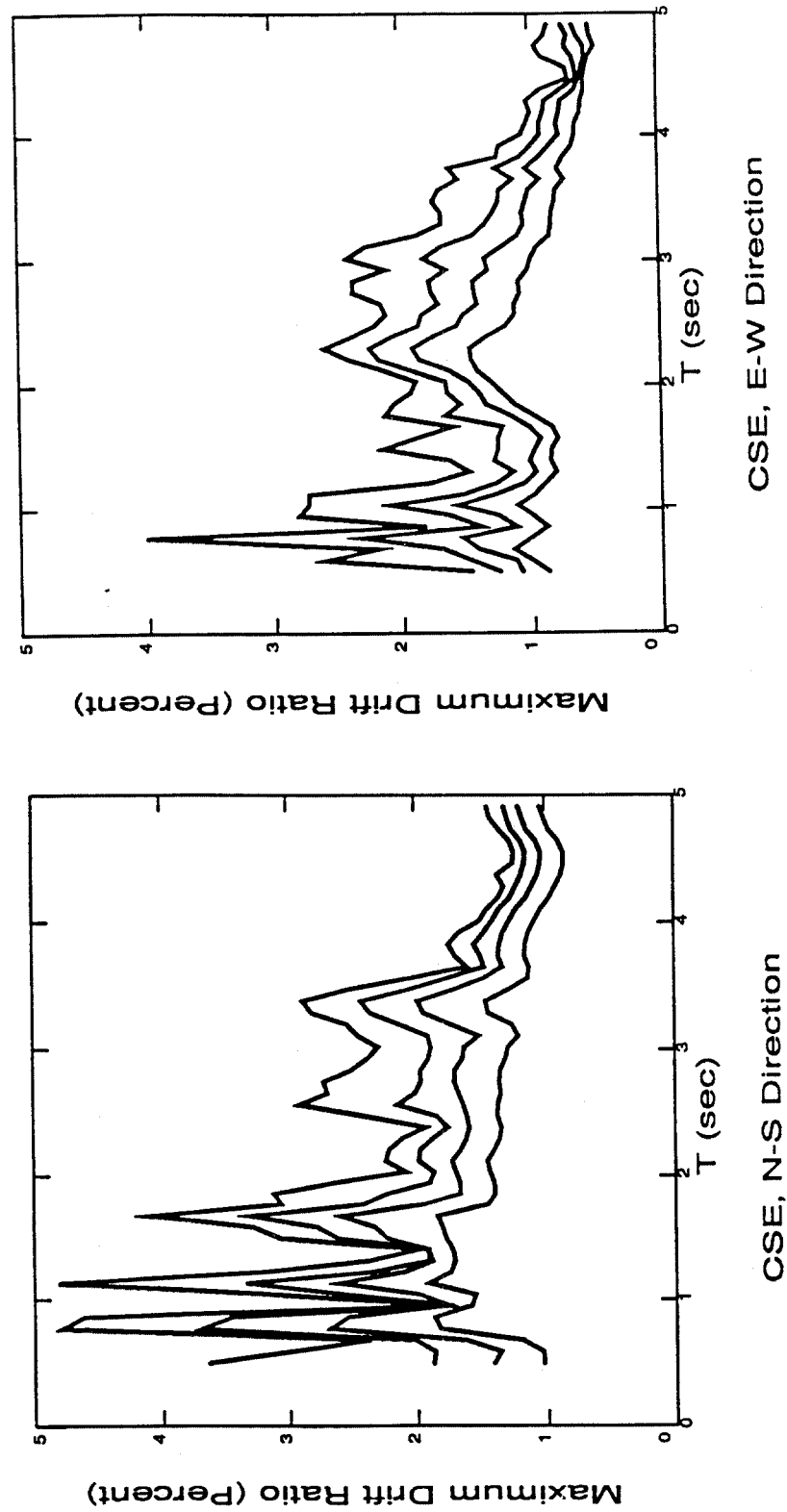
Drift Demand Spectra for Selected Northridge Sites

FIGURE 2-19: DRIFT DEMAND SPECTRA. 0, 2, 5, AND 10% DAMPING. SCS



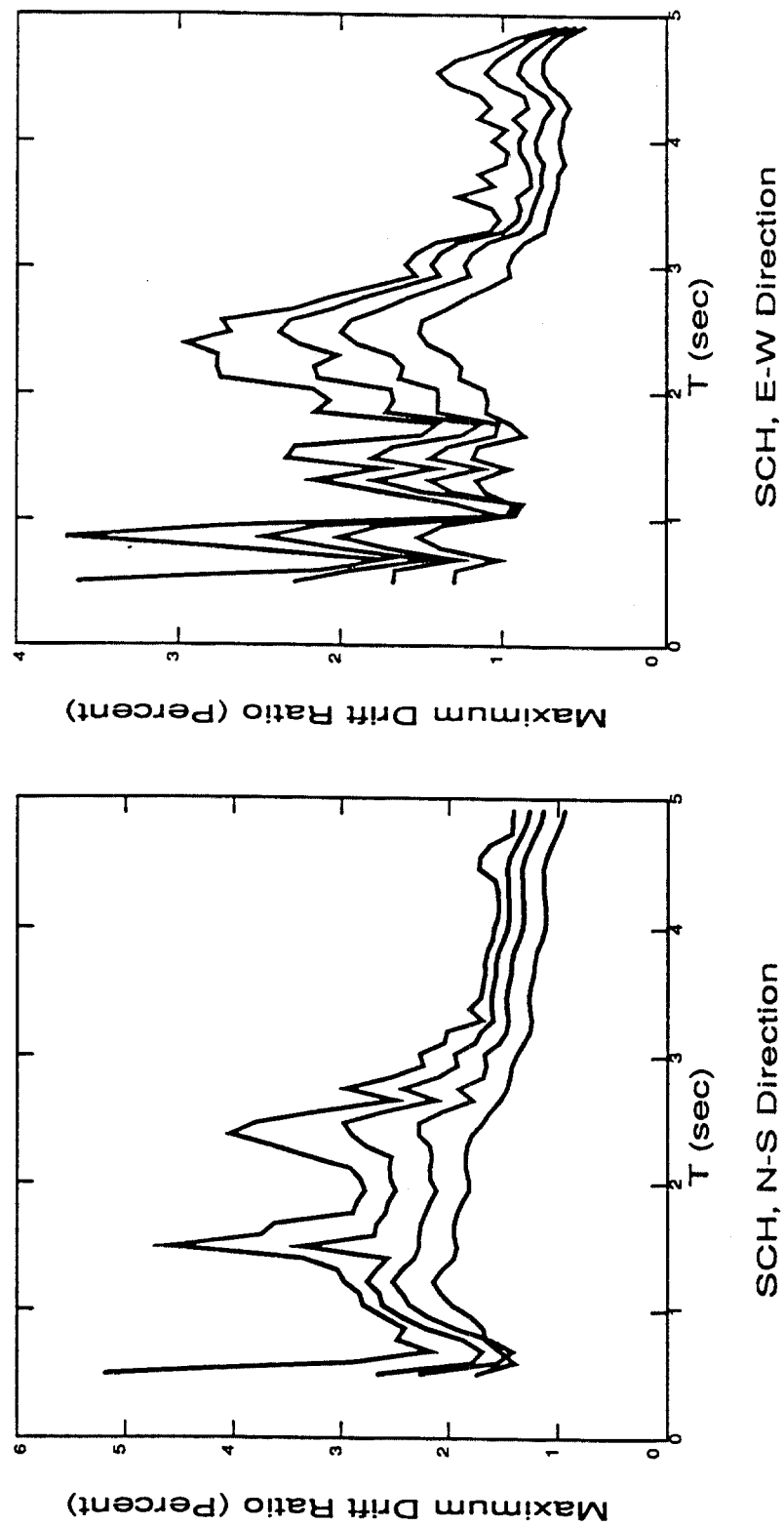
Drift Demand Spectra for Selected Northridge Sites

FIGURE 2-20: DRIFT DEMAND SPECTRA. 0, 2, 5, AND 10% DAMPING. CSE



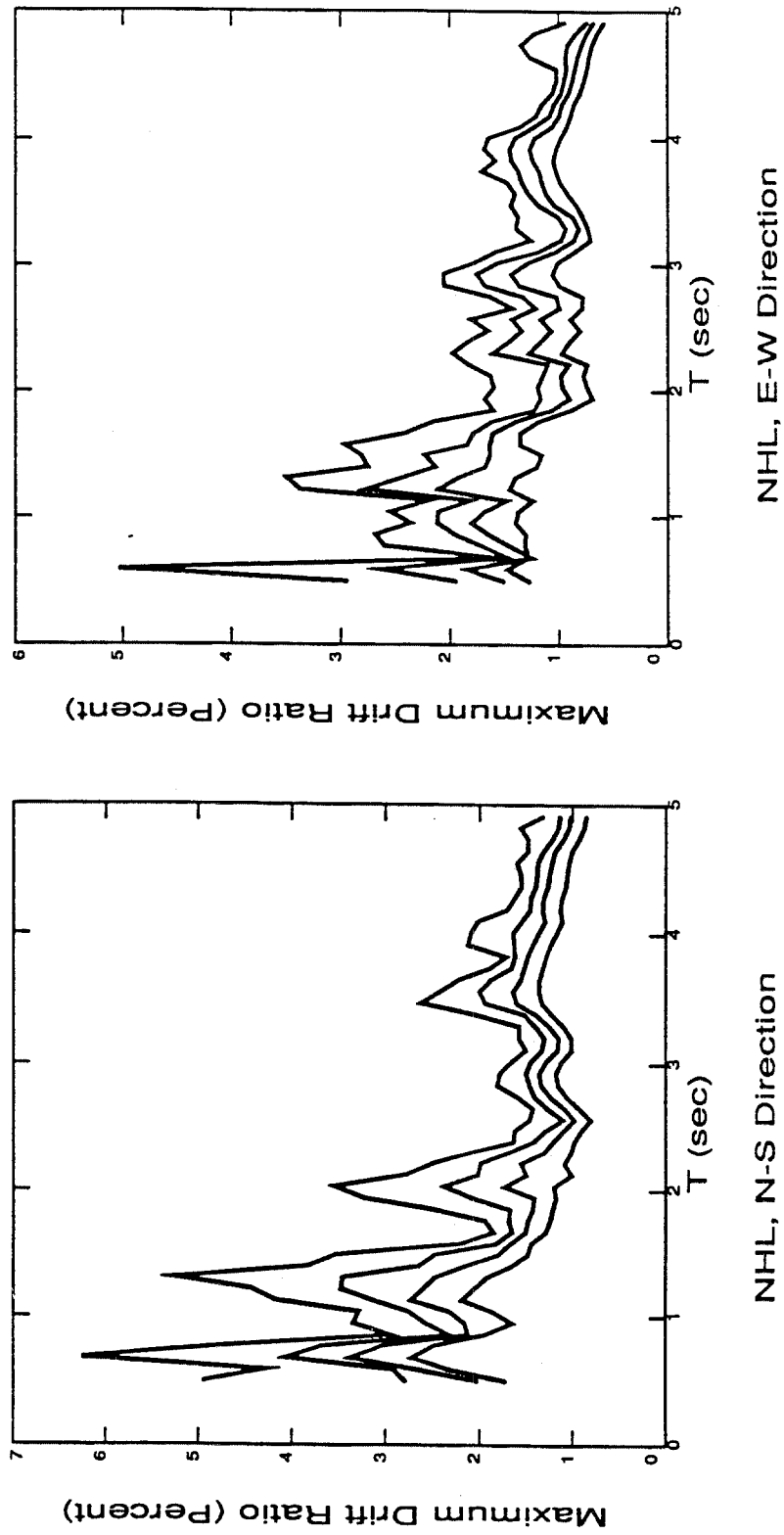
Drift Demand Spectra for Selected Northridge Sites

FIGURE 2-21: DRIFT DEMAND SPECTRA. 0, 2, 5, AND 10% DAMPING. SCH



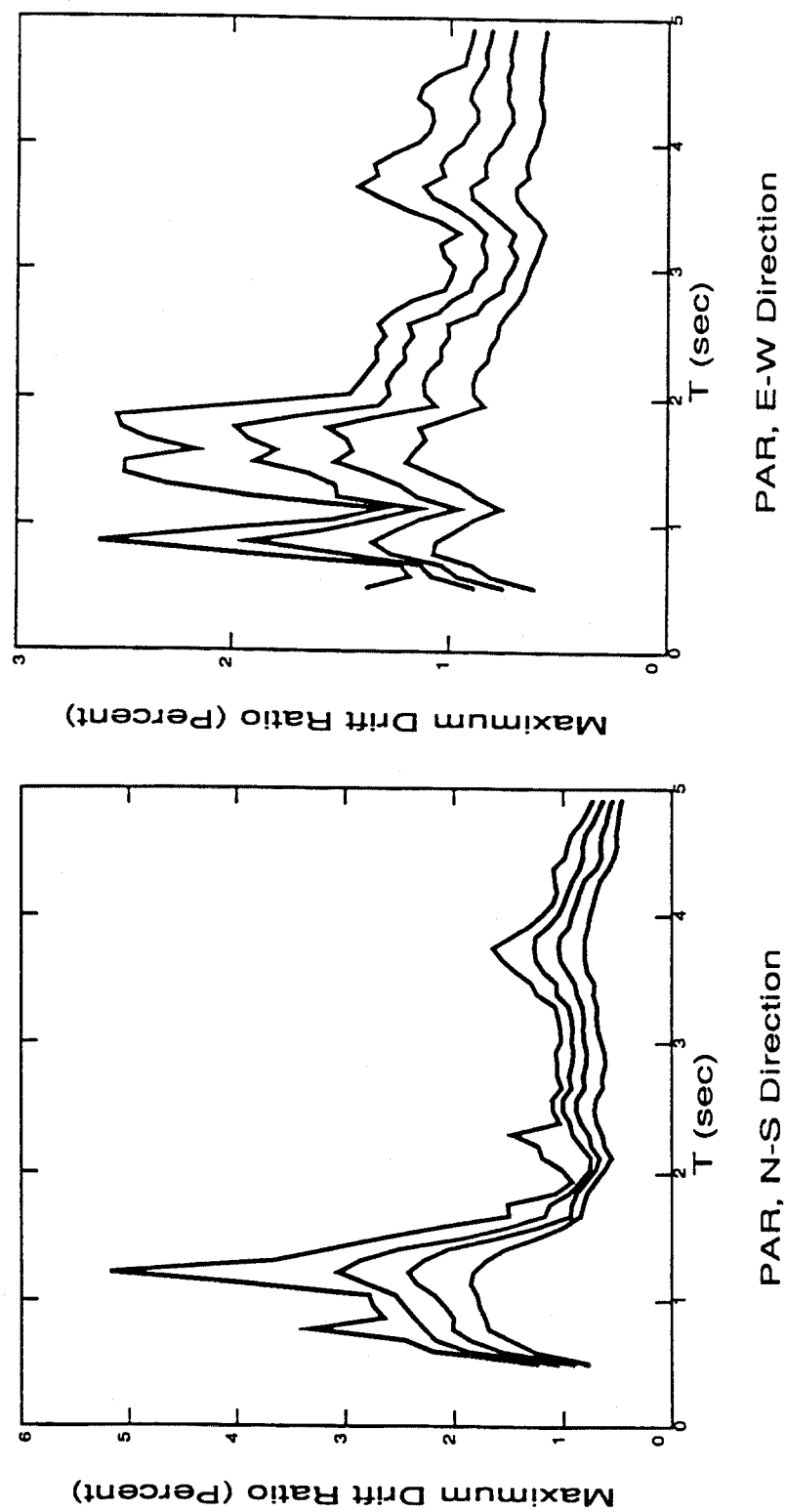
Drift Demand Spectra for Selected Northridge Sites

FIGURE 2-22: DRIFT DEMAND SPECTRA. 0, 2, 5, AND 10% DAMPING. NHL



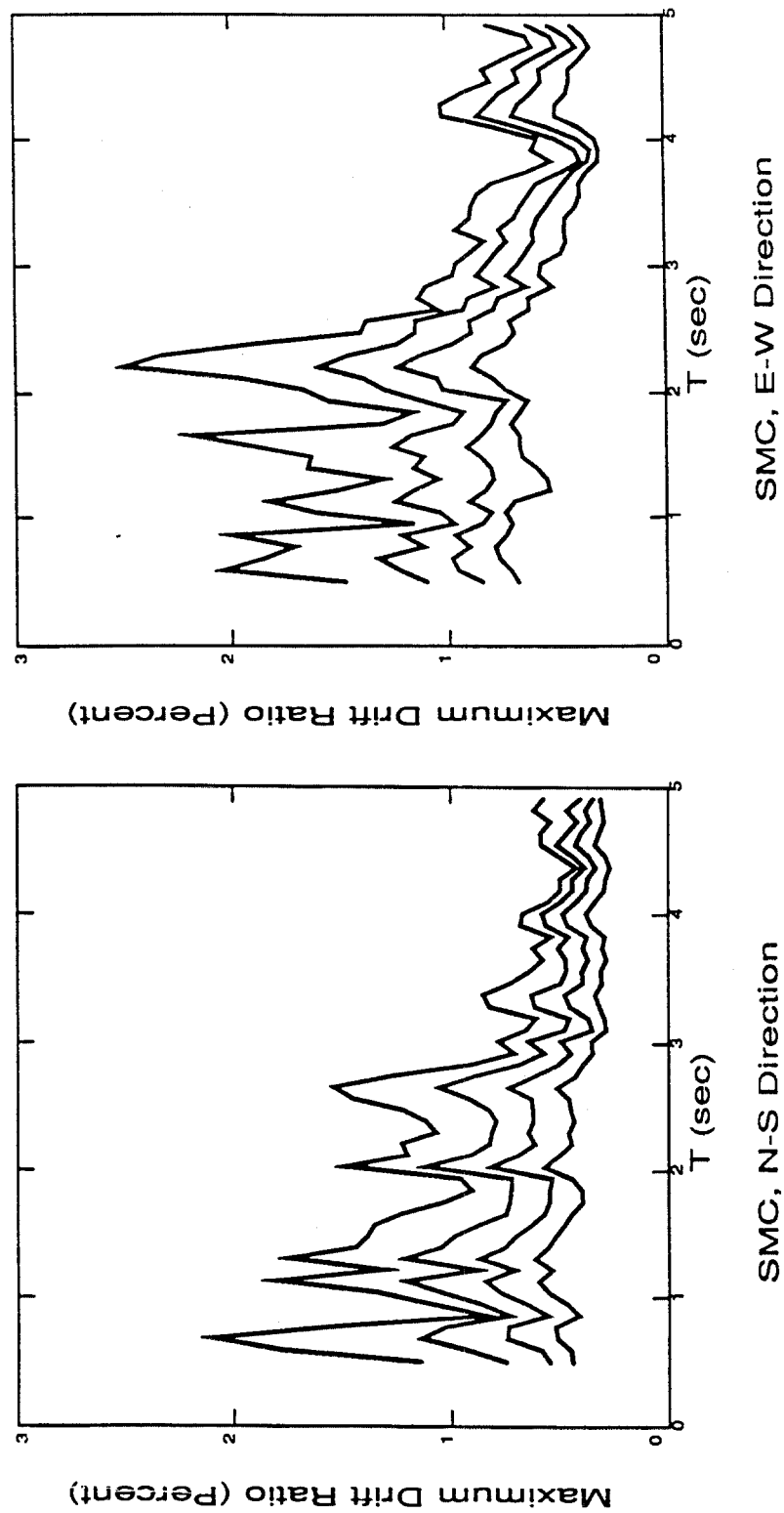
Drift Demand Spectra for Selected Northridge Sites

FIGURE 2-23: DRIFT DEMAND SPECTRA. 0, 2, 5, AND 10% DAMPING. PAR



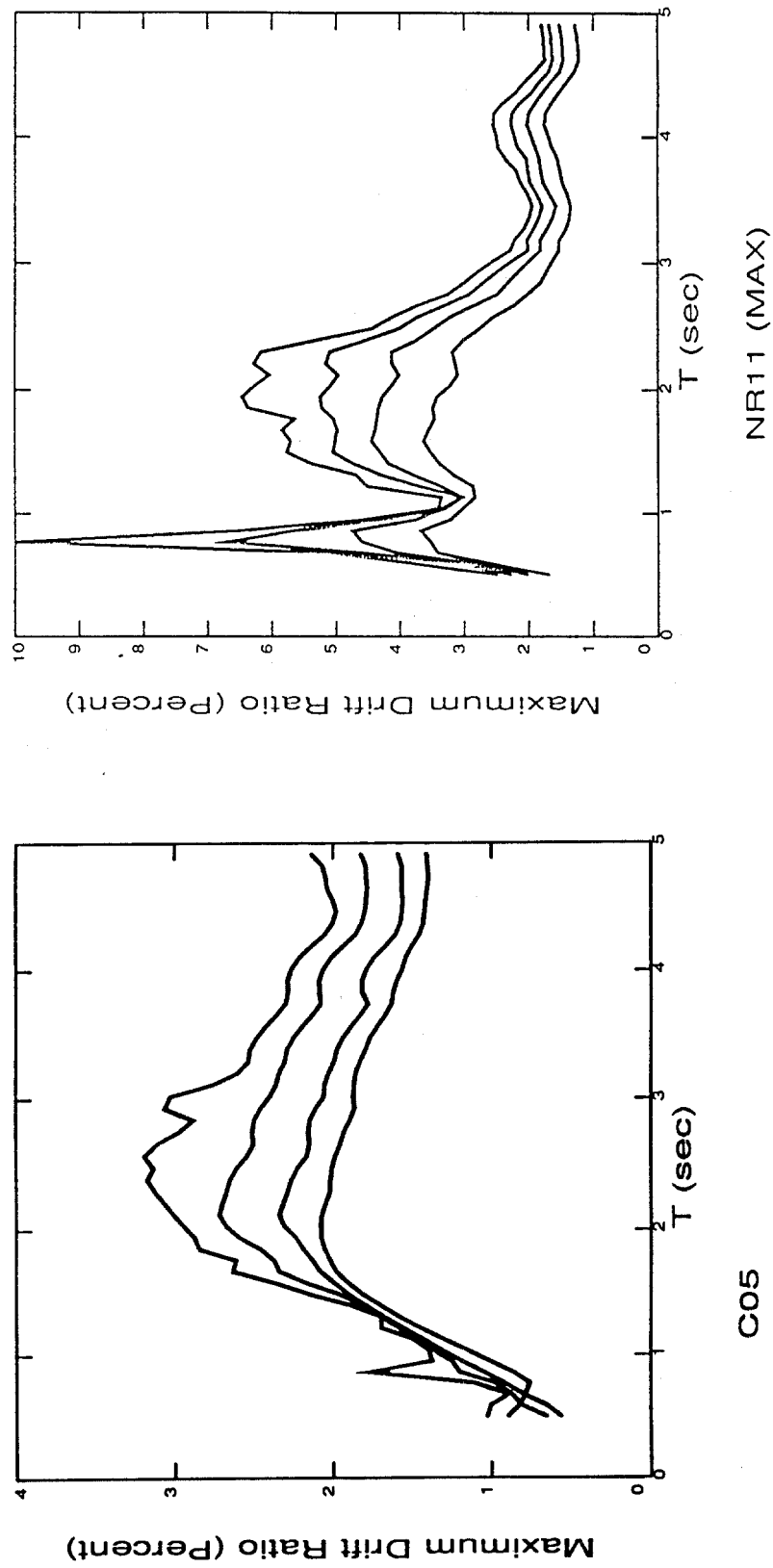
Drift Demand Spectra for Selected Northridge Sites

FIGURE 2-24: DRIFT DEMAND SPECTRA. 0, 2, 5, AND 10% DAMPING. SMC



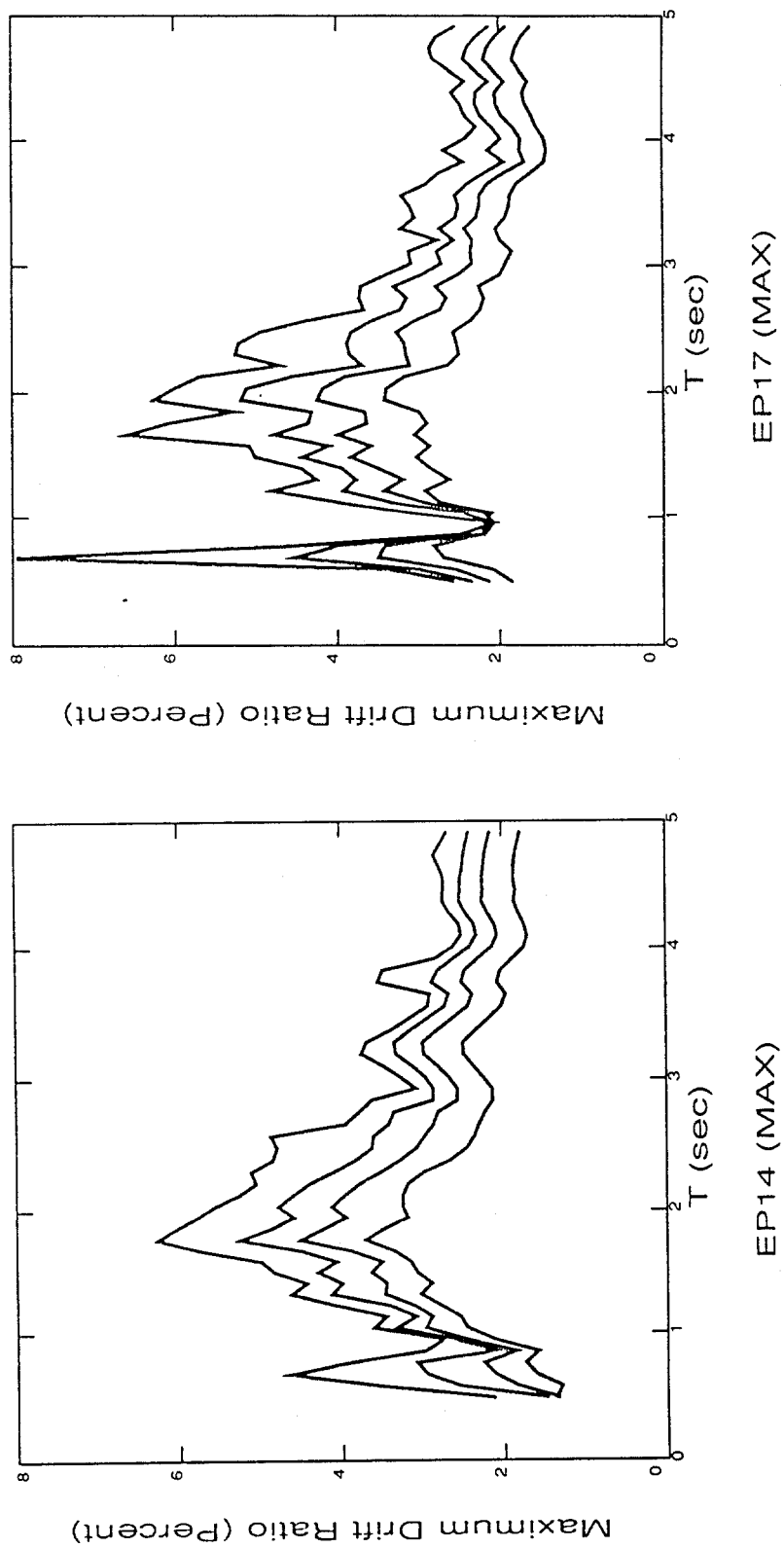
Drift Demand Spectra for Selected Northridge Sites

FIGURE 2-25: DRIFT DEMAND SPECTRA. 0, 2, 5, AND 10% DAMPING. NR11 AND C05. MAXIMUM VELOCITY
CHANGE DIRECTION



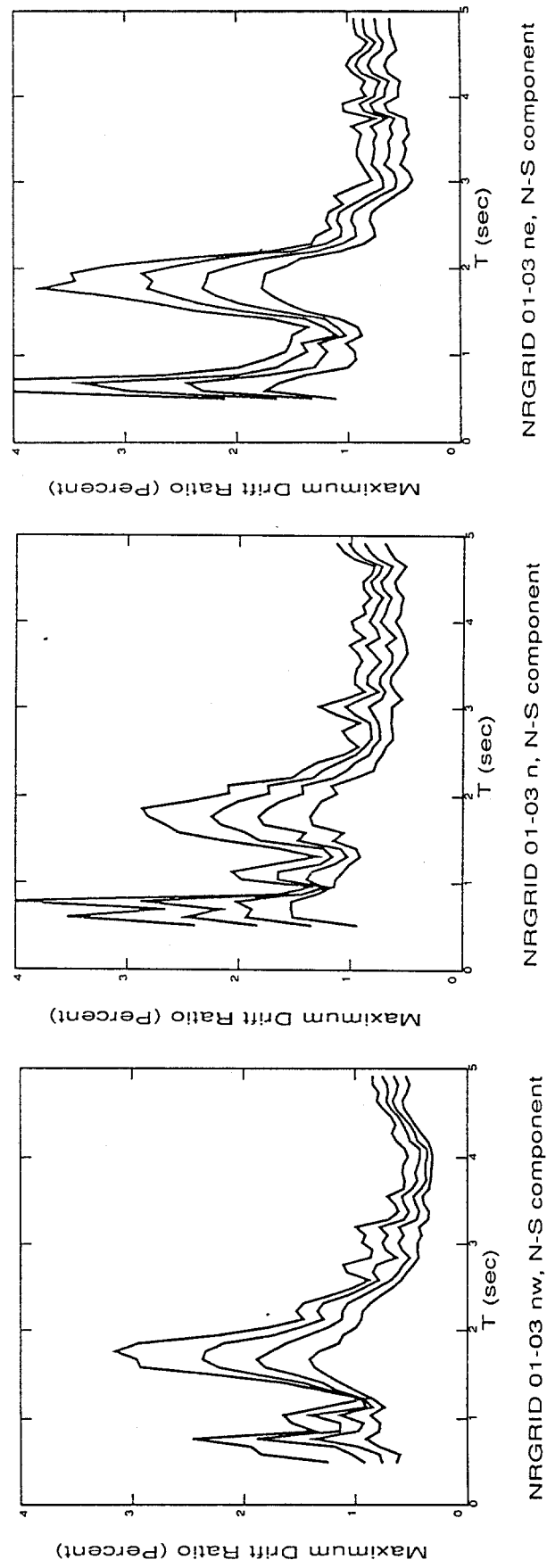
Drift Demand Spectra for Selected Northridge Sites

FIGURE 2-26: DRIFT DEMAND SPECTRA. 0, 2, 5, AND 10% DAMPING. EP14 AND EP17. MAXIMUM VELOCITY CHANGE DIRECTION



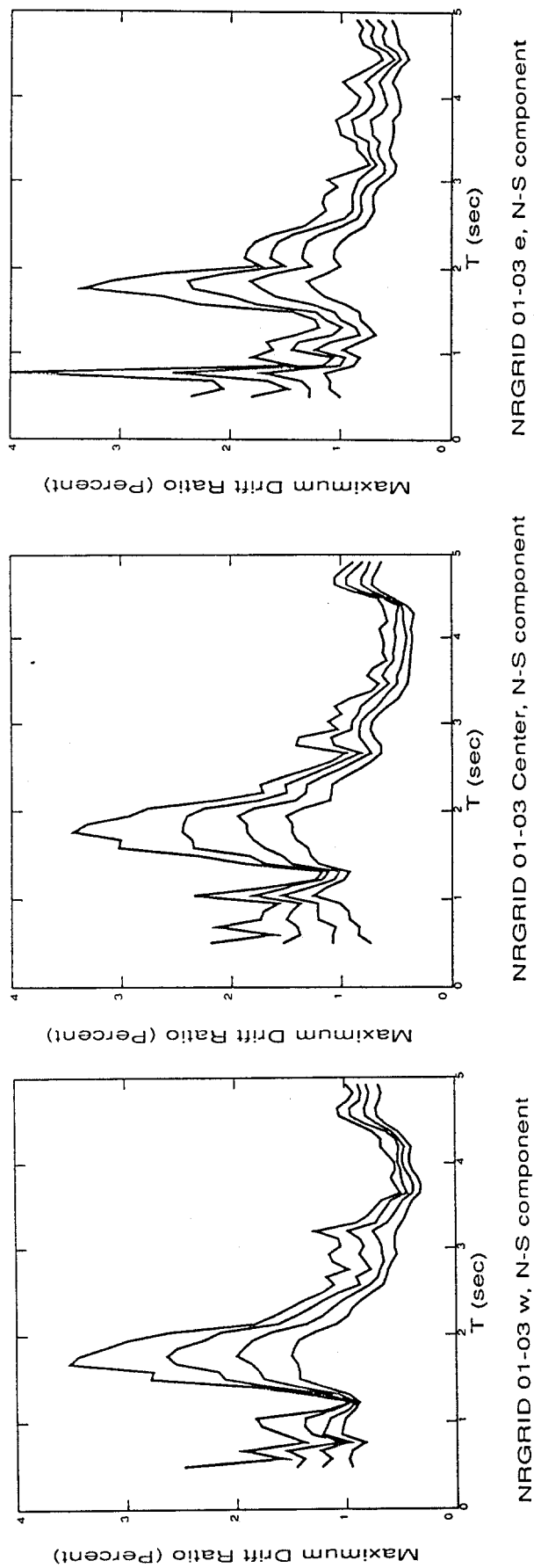
Drift Demand Spectra for Selected Northridge Sites

FIGURE 2-27: DRIFT DEMAND SPECTRA. 0, 2, 5, AND 10% DAMPING. NRGRD 01-03; NW, N, NE; N-S
DIRECTION



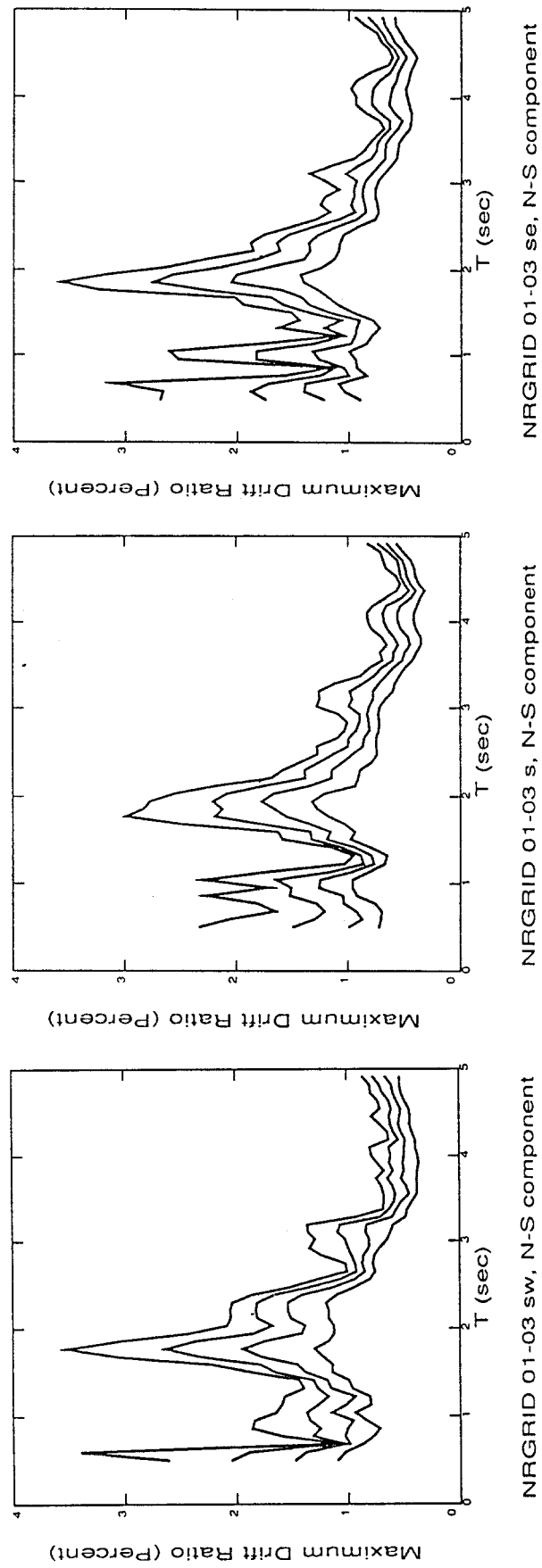
Drift Demand Spectra for Selected Northridge Sites

FIGURE 2-28: DRIFT DEMAND SPECTRA. 0, 2, 5, AND 10% DAMPING. NRGRD 01-03; W, C, E; N-S DIRECTION



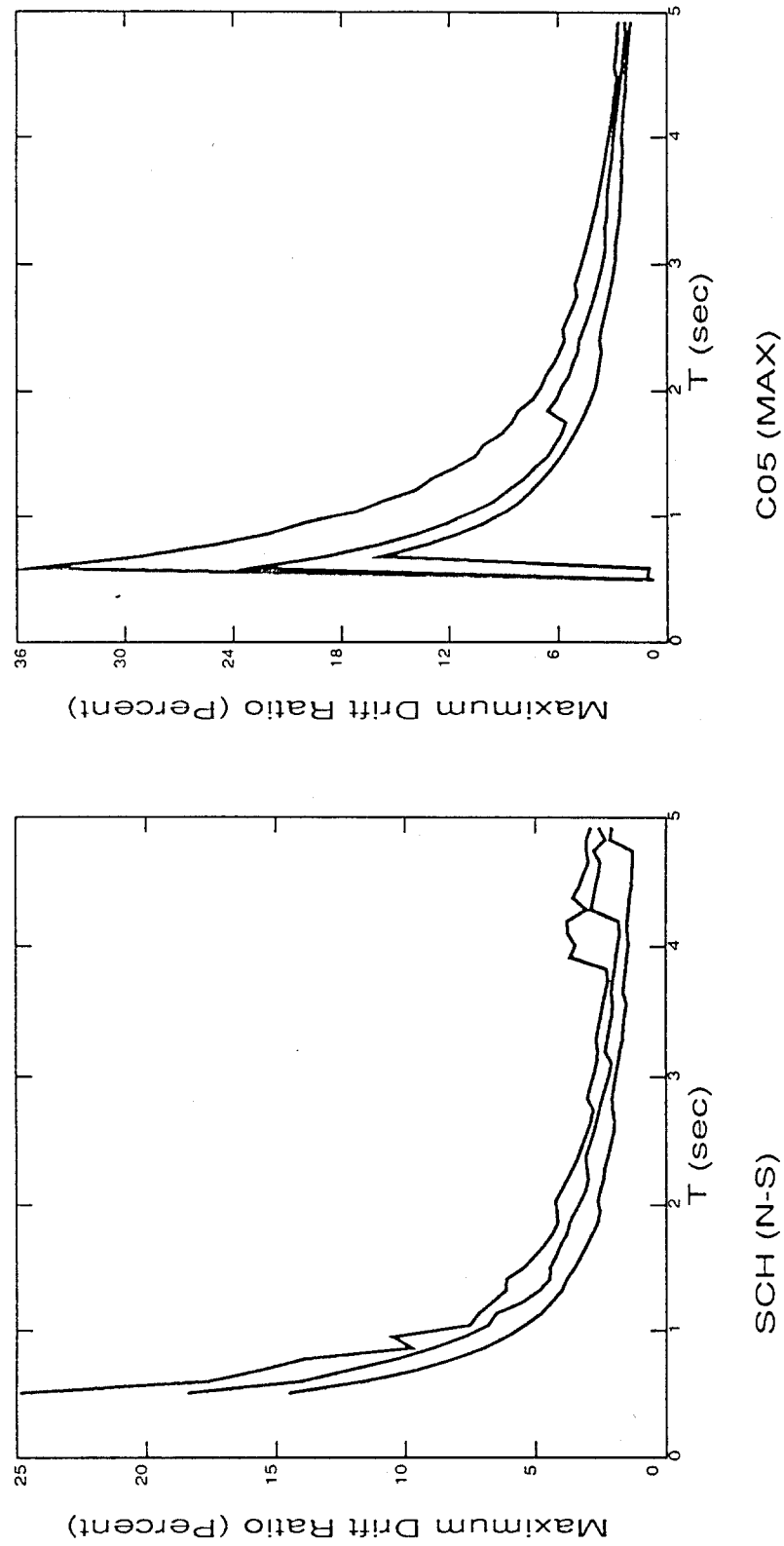
Drift Demand Spectra for Selected Northridge Sites

FIGURE 2-29: DRIFT DEMAND SPECTRA. 0, 2, 5, AND 10% DAMPING. NRGRD 01-03; SW, S, SE; N-S DIRECTION



Drift Demand Spectra for Selected Northridge Sites

FIGURE 2-30: DUCTILITY-BASED DRIFT DEMAND SPECTRA. 2, 5, AND 10% DAMPING. SCH (N-S) AND C05 9(MAX). MAXIMUM VELOCITY CHANGE DIRECTION



Drift Demand Spectra for Selected Northridge Sites

APPENDIX A

The following is extracted from the author's referenced paper "Near-field Considerations in Specification of Seismic Design Motions for Structures," which is to appear in the Proceedings of the 10th European Conference on Earthquake Engineering, Vienna, Austria, 1994. It is reproduced here because the Proceedings are not yet available.

A linear continuous shear-beam model has long been used to study the response of taller buildings. Such a model is employed herein to examine the effect of near-field velocity pulses on structural drift demand. The response of real buildings in the damage range will likely be nonlinear. However, studies have shown that the overall displacement response of a nonlinear hysteretic system to earthquake excitation is often well predicted by an equivalent linear system.

Consider the simple shear-beam building model shown in **Figure 2-A1**. Let the shear wave velocity in the building be c (m/s) and the height of the building be H (m). Then, the fundamental period, T , of the building will be $T = 4H / c$. From the Uniform Building Code (ICBO 1994), the period of a *steel* building may be related to its height as $T = 0.0853 H^{3/4}$. Assuming an effective story height of 3.6 m, the period and wave speed can both be determined in terms of the number of stories, N .

When a velocity time history, $v(t)$, is applied to the base of the shear-beam building model, the strain (inter-story drift ratio) at any location in the building can be calculated by the superposition of upward and downward traveling waves in the beam. The maximum drift will generally occur at the base of the structure. It can be shown that the maximum inter-story base drift ratio can be expressed approximately as

$$D_{\max} = \max_{\forall t} \frac{1}{c} \left| v(t) + 2 \sum_{n=1}^{n \leq 2t/T} (-1)^n (1 - \pi\zeta/2)^{2n} v(t - Tn/2) \right|$$

where ζ is approximately the damping in the first mode of response. By neglecting wave reflections, an asymptotic lower bound on the maximum drift for large N may be obtained as

$$D_{\max} \geq 0.015 v_{\max} / N^{1/4}$$

where v_{\max} (m/s) is the maximum ground velocity.

The inter-story drift demand, D_{\max} may be graphed as a function of either the building number of stories, N , height, H , or period, T , for different levels of damping, ζ . This representation will be referred to as the *drift demand spectrum*, or simply the *drift spectrum*. It is analogous to the response spectrum which gives the maximum displacement, velocity, or acceleration as a function of building period.

REFERENCES

- Iwan, W.D., 1980. "Estimating Inelastic Response Spectra from Elastic Spectra," *Earthq. Engr. and Struc. Dyn.*, Vol. 8, pp. 375-388, John Wiley and Sons, Ltd.
- Iwan, W.D., 1994. "Near-Field Considerations in Specification of Seismic Design Motions for Structures," *Proc. 10th European Conf. on Earthq. Engr.*, Aug. 28-Sept. 2, 1994, Vienna, Austria.
- Iwan, W.D. and X. Chen, 1994. "Important Near-Field Ground Motion Data from the Landers Earthquake," *Proc. 10th European Conf. on Earthq. Engr.*, Aug. 28-Sept. 2, 1994, Vienna, Austria.

ACKNOWLEDGMENTS

Funding for this research was provided by the Federal Emergency Management Agency through the SAC Joint Venture. SAC is a partnership of the Structural Engineers Association of California, the Applied Technology Council, and California Universities for Research in Earthquake Engineering.

FIGURE 2-A1.: SIMPLE SHEAR-BEAM BUILDING MODEL.

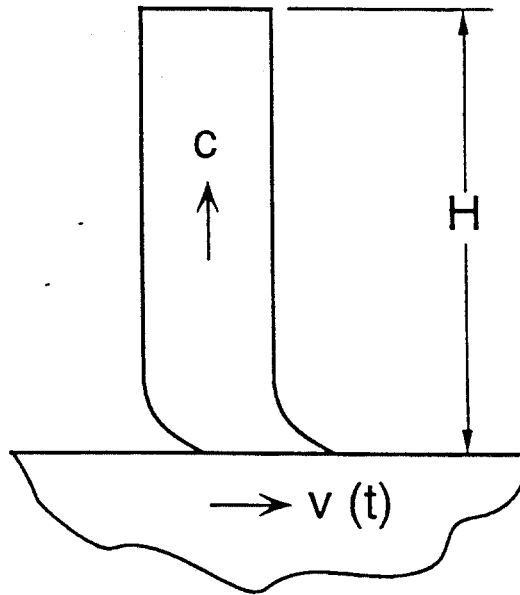


Figure 13. Simple Shear-Beam Building Model